TURUN
YLIOPISTO
UNIVERSITY
OF TURKU

FIBER-REINFORCED COMPOSITE WITH INTERPENETRATING POLYMER NETWORK

Influence of shelf-life of the prepreg and the adhesive primer on interfacial adhesive strength of the composite to a resin luting material

Aftab Ahmed Khan

TURUN YLIOPISTON JULKAISUJA – ANNALES UNIVERSITATIS TURKUENSIS
SARJA – SER. D OSA – TOM. 1541 | MEDICA – ODONTOLOGICA | TURKU 2021

TURUN
YLIOPISTO
UNIVERSITY
OF TURKU

FIBER-REINFORCED COMPOSITE WITH INTERPENETRATING POLYMER NETWORK

Influence of shelf-life of the prepreg and the adhesive primer on interfacial adhesive strength of the composite to a resin luting material

Aftab Ahmed Khan

TURUN YLIOPISTON JULKAISUJA – ANNALES UNIVERSITATIS TURKUENSIS
SARJA – SER. D OSA – TOM. 1541 | MEDICA – ODONTOLOGICA | TURKU 2021

University of Turku

Faculty of Medicine
Institute of Dentistry
Department of Biomaterials Science
Finnish Doctoral Program in Oral Sciences

Supervised by

Professor Pekka K Vallittu
Department of Biomaterials Science
Institute of Dentistry
University of Turku
Turku, Finland

Docent Eija Säilynoja
Department of Biomaterials Science
Institute of Dentistry
University of Turku
Turku, Finland

Reviewed by

Professor Marco Stephan Cune
University of Groningen
University Medical Center Groningen
Center for Dentistry and Oral Hygiene
Department of Restorative Dentistry and Biomaterials
Groningen, The Netherlands

Associate Professor Marco Bottino
Department of Cariology, Restorative Sciences & Endodontics
School of Dentistry
University of Michigan
Michigan, USA

Opponent

Professor Martin Rosentritt
Faculty of Medicine
University of Regensburg
Regensburg, Germany

The originality of this publication has been checked in accordance with the university of Turku quality assurance system using the Turnitin Originality Check service.

ISBN 978-951-29-8404-6 (PRINT)
ISBN 978-951-29-8405-3 (PDF)
ISSN 0355-9483 (Print)
ISSN 2343-3213 (Online)
Painosalama Oy, Turku, Finland 2021

If I have seen further it is by standing on the shoulders of Giants.

Sir Isaac Newton

To my mentors, for infusing the curiosity of research in me

UNIVERSITY OF TURKU
Faculty of Medicine
Institute of Dentistry
Departrment of Biomaterials Science
AFTAB AHMED KHAN: Fiber-reinforced composite with interpenetrating polymer network – Influence of shelf-life of the prepreg and the adhesive primer on interfacial adhesive strength of the composite to a resin luting material
Doctoral Dissertation, 119 pp.
Finnish Doctoral Program in Oral Sciences
March 2021

ABSTRACT

Fiber-reinforced composite (FRC) is a low-cost metal-free restorative alternative. To overcome problems related to the interfacial adhesion between composite luting material and FRC, a semi-interpenetrating polymer network (semi-IPN) matrix with linear polymer of poly(methylmethacrylate) (PMMA) was developed for FRC. Therefore, a series of laboratory studies were executed to investigate the effect of shelf-life, monomer systems and PMMA gradient on the intact and ground substrates of semi-IPN FRC.

In the four experimental studies, everStick C&B was used as the semi-IPN based FRC. The first study evaluated the shelf-life and dissolving capability of the methyl methacrylate (MMA) monomer in polymerized FRC. The second study investigated the effect of different adhesive/primer on polymerized FRC which were stored for various durations (at 4°C; 1.0, 1.5, and 3-year) before curing. The third study analyzed the tensile bond strength (TBS) between resin luting material and FRC using different adhesive/primers systems. The fourth study determined TBS between polymerized FRC intact (high gradient PMMA) or ground (low gradient PMMA) surfaces and a resin luting material. The results were statistically analyzed using analysis of variance (ANOVA), the *post hoc* Tukey's test, regression and correlation analysis using statistical software.

It can be concluded that upon aging, the linear and cross-linked components of the semi-IPN structure of FRC might become phase-segregated. Both G-Multi PRIMER and Composite Primer might have the ability to diffuse into polymerized FRC and form a durable adhesive layer with increased nanohardness and adhesive strength between resin luting material and the FRC substrate. The highest TBS can be achieved for FRC intact surface treated with the G-Multi PRIMER.

KEYWORDS: Adhesive interface, Fiber-reinforced composite, Nanohardness, Tensile bond strength, Semi-interpenetrating polymer network, Monomer, Primer

TURUN YLIOPISTO
Lääketieteellinen tiedekunta
Hammaslääketieteen laitos
Biomateriaalitiede
AFTAB KHAN: Osittaislomittaismuoviverkostorakenne kuitulujitteissa muovissa – muovin esivalmisteen säilytysajan ja pinnan esikäsittelyajan vaikutus muovin rajapintaliitoksen sidoslujuuteen. Väitöskirja, 119 s.
Suun terveystieteiden tohtoriohjelma (FINDOS-Turku)
maaliskuu 2021

TIIVISTELMÄ

Kuitulujittenen muovi on hammashoidon materiaali, joka täyttää hammaslääketieteen asettamat ulkonäölliset ja lujuusvaatimukset. Kuitulujitteinen muovi koostuu lujitekuiduista ja niitä sitovasta yleensä ristisilloitetusta muovimatriisista, joka voi olla myös osittaislomittaisverkostomuovirakenne (engl. semi-IPN). Tässä tutkimuksessa selvitettiin kuitulujite-esivalmisteen säilytysajan ja kovetetun kuitulujiteteisen muovin pinnan esikäsittelyn vaikutusta muovin liimautumiseen muihin hammaslääketieteessä käytettyihin muoveihin.

Tutkimuksessa käytettiin semi-IPN muovipitoista kuitulujitteista muovia. Kuitulujitteisen muovin pinnan rakennetta ja ominaisuuksia tutkittiin muovin kovettamisen jälkeen. Vertailua tehtiin muun muassa nanomekaanisella pinnan analysoinnilla niistä muoveista, joiden esivalmistetta oli säilytetty jopa kaksi vuotta ennen näytteen valmistusta. Lisäksi tutkimuksessa kiinnitettiin erityistä huomiota kuitulujitteisen muovin liimautumiseen toiseen muoviin ja tällöin verrattiin erilaisten pinnan esikäsittelyaineiden vaikutusta rajapintaliitoksen sidoslujuuteen.

Tulokset osoittivat tilastollisesti merkitseviä eroja näytteen pinnan nanokovuudessa pinnan eri kerrossyvyyksissä, mikä osoittaa semi-IPN gradienttirakenteen olemassaolon. Käytetyt kaksi esikäsittelyainetta saivat rajapintaliitoksen pinnan kovuuden lisääntymään näytteissä, jotka oli valmistettu tuoreesta kuitulujitteisen muovin esivalmisteesta. Myös esivalmisteen säilytysaika ennen sen käyttämistä vaikutti merkitsevästi liimautumiseen. Korkein sidoslujuus saavutettiin kuitulujitteisella muovilla, jonka pintaa ei oltu hiottu ennen liimaamista eli pinnan gradienttirakennetta ei oltu poistettu.

AVAINSANAT: kuitulujitteinen muovi, sidosulujuus, sidostaminen, yhdistelmä muovi, esikäsitteluaine.

Table of Contents

Abbreviations

Al_2O_3	Aluminium oxide
ANOVA	Analysis of variance
ATR	Attenuated total reflectance
*bis*GMA	Bisphenol-A-glycidyl methacrylate
B_2O_3	Boron oxide
CaO	Calcium oxide
cm^{-1}	Wavenumber
cm^2	Square centimeter
DC	Degree of conversion
DSC	Differential scanning calorimetry
EGDMA	Ethylene glycol dimethacrylate
FRC	Fiber-reinforced composites
FTIR	Fourier-transform infrared spectroscopy
GPa	Gigapascal
h	Hour
IPN	Interpenetrating polymer network
kPa	Kilopascal
kV	Kilovolt
mg	Milligram
MgO	Magnesium oxide
min	Minute
mL	Milliliter
mm	Millimeter
mm^3	Cubic millimeter
MMA	Methyl methacrylate
MPa	Megapascal
mN	Millinewton
mW	Milliwatts
MW	Molecular weight
nm	Nanometer
Pa	Pascal

PEGDMA	Polyethylene glycol dimethacrylate
PMMA	Poly(methyl methacrylate)
rpm	Revolutions per minute
s	Second
SEM	Scanning electron microscopy
SiO_2	Silicon dioxide
TBS	Tensile bond strength
TEGDMA	Triethylene glycol dimethacrylate
T_g	Glass-transition temperature
TGA	Thermogravimetric analysis
THF	Tetrahydrofuran
UDMA	Urethane dimethacrylate
µg	Microgram
UHMWPE	Ultrahigh molecular weight polyethylene
µm	Micrometer
VHN	Vickers hardness number
Vol.	Volume
Wt.	Weight
XRD	X-ray diffraction

List of Original Publications

This dissertation is based on the following original publications, which are referred to in the text by their Roman numerals:

I. **Khan AA.,** Al-Kheraif AA., Al-Shehri AM., Säilynoja E., Vallittu PK. Polymer matrix of fiber-reinforced composites: Changes in the semi-interpenetrating polymer network during the shelf life. J Mech Behav Biomed Mater 2018; 78: 414–19. doi: 10.1016/j.jmbbm.2017.11.038.

II. **Khan AA.,** Al-Kheraif AA., Mohamed BA., Perea-Lowery L., Säilynoja E., Vallittu PK. Influence of primers on the properties of the adhesive interface between resin composite luting cement and fiber-reinforced composite. J Mech Behav Biomed Mater 2018; 88: 281–87. doi: 10.1016/j.jmbbm.2018.08.050.

III. **Khan AA.,** Mohamed BA., Al-Shamrani SS., Ramakrishnaiah R., Perea-Lowery L., Säilynoja E., Vallittu PK. Influence of monomer systems on the bond strength between resin composites and polymerized fiber-reinforced composite upon aging. J Adhes Dent 2019; 21: 509–16. doi: 10.3290/j.jad.a43610.

IV. **Khan AA.,** Perea-Lowery L., Al-Kheraif AA., Eldwakhly E., Säilynoja E., Vallittu PK. Interfacial adhesion of a semi-interpenetrating polymer network-based fiber-reinforced composite with a high and low-gradient poly(methyl methacrylate) resin surface. Polymers 2021; 13: 352(1–9). doi: 10.3390/polym13030352

1 Introduction

With the advanced technology available today, dental biomaterials are constantly evolving. The development of new biomaterials offers various solutions to many complex oral problems. Increased demand for esthetically pleasing dental materials has led to the exploration of metal-free prosthetic alternatives. The introduction of fiber-reinforced composites (FRC) has replaced metallic materials for periodontal splints (Khan et al., 2018b), root canal posts (Vallittu, 2018), orthodontic devices (Scribante et al., 2018a), as well as removable and fixed prostheses (Zhang and Matinlinna, 2012).

FRCs offer high stiffness and strength per unit of weight. Typical FRC materials are made of highly cross-linked polymer matrix that is reinforced by micrometer scale glass fibers. In directly made FRC restorations, the bonding between veneering composite, adhesives and FRC substructure is based on free radical polymerization of the resin luting material to the resin matrix of FRC. However, in indirectly made FRC restorations such as posts or repairs of fixed partial dentures, the adhesion mechanism relies entirely on micromechanical interlocking or utilization of exposed glass fiber surfaces. Besides, exposed glass fibers require chairside silanization, which has been shown to be prone to weakening by hydrolysis (Vallittu and Özcan, 2017; Heikkinen et al., 2013)

To overcome problems associated with the interfacial adhesion between resin luting material and polymerized FRC, a semi-interpenetrating polymer network (semi-IPN) matrix was developed as a matrix system for FRC. Semi-IPN based FRC is a new class of materials which contains a combination and precise volumes of cross-linked bisphenol-A-glycidyl methacrylate (*bis*GMA) or triethylene glycol dimethacrylate (TEGDMA) and linear poly(methyl methacrylate) (PMMA). The advantages of these two independent polymer networks, not linked by chemical bonding, is that the presence of enriched quantity of linear polymer on FRC surface provides the possibility to be dissolved by the monomer system of the resin luting material, and hence improved bonding between the substrates. The dissolving depth of the monomer is governed by its solubility parameters, monomer interaction time with the FRC substrate, room temperature at which monomer interacts with the FRC, and polymeric contents of semi-IPN-based FRC structures (Chen et al., 1998).

A few important aspects remain, *i.e.*, monomer system of the adhesive/primer and resin luting materials, shelf-life of FRC and FRC with high and lower PMMA gradients, which have not been studied in detail. The effect that different monomer systems have on the mechanical and bonding properties of the secondary-IPN, *i.e.* the IPN layer between veneering/resin luting material and semi-IPN polymer matrix FRC (Vallittu, 2009) formed due to the dissolving capability of monomers of the adhesive/primer and resin luting material has also not yet been thoroughly explored. Therefore, the work described in this thesis focuses on studying the mechanical properties of the secondary-IPN (weakest link between resin luting material and semi-IPN based FRC).

2 Review of the Literature

2.1 Fiber-reinforced composite (FRC)

2.1.1 Introduction and background

A composite material is made of two or more materials, which differ in shape and composition with significantly different physical or chemical properties. When constituent materials with different properties are combined, the materials neither merge nor do they dissolve or react. However, they form a new material with characteristics different from its individual components. The individual components maintain their properties and are linked together with an interface in the form of a composite material (Van Noort and Barbour, 2014).

Fiber-reinforced composite (FRC) is a synthetic material combination which consists of two different components: the matrix (continuous phase) and the fibers (dispersed phase) (Scribante et al., 2018a; Vallittu and Matinlinna, 2017).

Despite wide clinical use of particulate-reinforced composite (PRC) in recent years, there still exists many drawbacks of PRC such as poor fatigue and wear behaviors, polymerization shrinkage, and vulnerability to chemical degradation in the oral cavity that negatively influences the clinical performance of the material (Oberholzer et al., 2007; Başaran et al., 2013). Moreover, in clinical situations where a material with enhanced levels of strength is necessary and esthetics is important (Conrad et al., 2007), the conventional PRC becomes far from ideal. The desire to find a metal-free restorative material that withstands highly-demanding clinical situations motivated further investigation for a more durable material with higher strength and improved esthetics.

2.1.2 History of FRCs in dentistry

Although, subsequent developments in dental composites have taken place over time, *i.e.*, from microfill to bulk-fill composites, chipping and bulk fracture have prevented their use in high-stress–bearing areas. However, the introduction of engineering techniques in the dental field, *i.e.*, 'Fiber-reinforcing Technology' has improved the mechanical properties of dental composites. Using better engineering techniques, fillers with a high aspect ratio (the ratio between the length and diameter

of the filler) act as a supporting/reinforcing component to the overlay composite material, if the fibers are precisely oriented, carefully incorporated and well-bonded with the resin component (Landel and Nielsen, 1993; Vallittu and Matinlinna, 2017).

In the early 1960s and 1970s, researchers attempted to reinforce PMMA dentures with glass fibers (Smith, 1962) or carbon fibers (Schreiber, 1974). In the middle of the 1980s, attempts were again made to fabricate fiber-reinforced prosthodontic frameworks for fixed prosthodontic restorations, implants, orthodontic retainers, and splints (Deboer et al., 1984; Grave et al., 1985). However, these materials and techniques mainly failed owning to intensive, difficult and cumbersome clinical manipulation procedures, and because of insufficient enhancement of their mechanical properties. Moreover, most of the suggested techniques involved the manual placement of fibers into resin systems. This approach was complicated and great care in handling and avoiding fibers from contamination was required during the impregnation process. The previous attempts mainly failed due to poor impregnation and wetting of the fiber bundles by the highly viscous resin systems, e.g., denture base resin with insufficient coupling or even gaps between the fibers and resin. Secondly, the use of 15% by volume fibers by hand placement was low compared to 50% or even as much as 70% by volume due to current industrial techniques.

In the late 1980s, the importance of the physical coupling of fibers to polymer matrix was recognized and therefore impregnation of the fiber bundles was performed either at chairside or in a laboratory manually by applying a low viscosity resin to the fiber bundles or alternatively the fiber bundles were pre-impregnated during a controlled manufacturing process (Goldberg and Burstone, 1992). The earliest pre-impregnated FRCs for dental applications were based on glass-reinforced thermoplastics. The subsequent FRCs were pre-impregnated with glass-reinforced polycarbonate as the framework for fixed partial dentures (Altieri et al., 1994). However, due to challenging manipulation and poor bonding of thermoplastic resin to tooth structure, the investigators targeted a *bis*GMA based resin system for the FRCs. Concurrently, there was ongoing research to use FRCs in denture base polymers based on PMMA. Denture base polymers are multiphase polymers of PMMA and partially cross-linked polymer matrix. For denture fabrication reasons, it is desired that the resin has a very high, dough-like viscosity when the resin is molded for denture base. Dough viscosity is far from optimal when used to impregnate reinforcing fibers. For denture base reinforcement, a system of polymer pre-impregnation was developed (Vallittu and Lassila, 1992; Vallittu, 1995a; Vallittu, 1995b; Vallittu, 1999).

Subsequently, the polymer pre-impregnated fiber system was combined with a light cured *bis*GMA polymer matrix and the first semi-IPN matrix FRC was available for dental use. This started active research on a dental semi-IPN system which is still ongoing and advancing (Kallio et al., 2001; Lastumäki et al., 2002; Lastumäki et al., 2003).

2.2 Current use of FRC in dentistry

The primary application of FRCs in dentistry is in prosthodontics and restorative dentistry. With FRC, fixed dental prostheses (FDP) can be achieved by minimally damaging the healthy tooth structure (Garoushi et al., 2008). FRCs can be utilized to repair the existing traditional prostheses. Veneers made of porcelain-fused-to-metal can also be repaired using woven glass fiber reinforcement (Özcan et al., 2006; Vallittu, 2002). Furthermore, conventional removable prostheses and those retained by attachment systems can also be reinforced using FRCs (Narva et al., 2001; Gibreel et al., 2019; Gibreel et al., 2018).

FRCs can be used in indirect pontic fabrication, also in combination with computer-aided design and computer-aided manufacturing based technologies (Perea et al., 2014). A report suggested that the FRC support could withstand chewing forces within the experimental period of 8.5 years (Strassler and Serio, 2007). Additionally, strength and resilience of FRC may support build-up of a 3-unit porcelain and FRC bridge (Garoushi and Vallittu, 2007). FRC fixed partial dentures can serve for 5–10 years (Feinman and Smidt, 1997). Very recently, a nine-year clinical follow-up study showed high survival times of direct FRC-based FPDs which is in line with earlier clinical studies and clinical experience (Perrin et al., 2020).

In conservative dentistry, the FRC substructure serves to support composite restoration and helps in crack-prevention due to its superior fracture toughness (Garoushi et al., 2007; Fráter et al., 2020; Bijelic-Donova et al., 2020). Usually the lost dentin is replaced using short FRCs and enamel with a surface layer of particulate filler composite resin (Scribante et al., 2018b). FRCs have biomimetic properties and can effectively be used as minimally invasive substitutes for missing hard dental tissues. They closely resemble the mechanical features and properties of natural teeth. FRC's polymerization shrinkage and depth of cure have been reported to be superior to conventional resin composites (Garoushi and Vallittu, 2007).

In the reconstruction of an endodontically treated tooth, FRC posts exhibit higher fracture endurance than those restored with only resin composite, and can provide increased bonding properties to resin cements (Khan et al., 2018d; Tanner et al., 2017). A Semi-IPN-based FRC post can offer secured bonding to resin luting materials and resin-based materials in general (Kallio et al., 2014; Le Bell et al., 2004; Le Bell et al., 2005; Lindblad et al., 2010; Le Bell-Rönnlöf et al., 2011).

In orthodontics, FRC-based fixed appliances used after orthodontic treatment are critical as the need to support the teeth in a correct position is pivotal for lasting clinical results. FRC's bond strength on enamel and on dentin is sufficient and clinically reliable, which is also favorable (Dj et al., 2009). In contemporary clinical practice, metallic arch wires are being replaced with FRC based wires for esthetic purposes. The clinical success of FRC resins has been documented for space maintaining purposes (Tayab et al., 2011). Also, the use of FRCs has been suggested as novel materials for

fabrication and bonding of brackets (Sfondrini et al., 2018; Shinya et al., 2008; Kilponen et al., 2019; Kilponen et al., 2016) and orthodontic wires (Inami et al., 2015; Ohtonen et al., 2013; Lucchese et al., 2018; Tanimoto et al., 2015).

The splinting of two tooth segments has also become possible using FRC. FRC splints have been shown to be able to resist higher flexural forces compared to conventional metallic wires (Cacciafesta et al., 2008). In pediatric dentistry, FRCs can be used in almost all the fields as described above (Beldüz Kara et al., 2018; Cauwels et al., 2014).

In oral and maxillofacial surgery, metallic implants are now being replaced with FRC because metal objects interfere with some medical imaging systems, and their stiffness differs from that of natural bone. The use of FRC-based orbital floor implants, cranioplasty implants, and craniofacial bone reconstruction are worth mentioning (Scribante et al., 2018b; Vallittu, 2017).

2.3 Fiber arrangement in FRC

Fibers maybe arranged in FRC structures in either continuous unidirectional form (rovings and yarns), continuous bidirectional form (weaves and fabrics), continuous random oriented (mat) or discontinuous (short and chopped) random or oriented fibers. Fibers can also be three-dimensionally oriented (Vallittu and Matinlinna, 2017). The effectiveness of fiber reinforcement technology is dependent on many variables including the type of resin used, the quantity of fibers in the resin matrix, fiber type, length, form, orientation, adhesion to the polymer matrix and impregnation of fibers with the resin (Vallittu, 2015; Edwards, 1998). The use of each type of fiber within FRC structures has its own properties and advantages over the other types. Unidirectional fibers provide anisotropic mechanical properties *i.e.*, mechanical properties in a single direction to the composite. Whereas, bi-directional fibers allow for multi-directional reinforcement of the restoration (Butterworth et al., 2003), thus effective when it is difficult to anticipate the direction of stress in the prosthesis, e.g. full crown. The clinician needs to be well aware of the advantages and limitations of each type of fiber to select the best FRC for a particular clinical situation. The strongest engineering materials are generally made of continuous unidirectional fibers (Vallittu and Matinlinna, 2017). The schematic presentation of fiber orientation is shown in Figure 1.

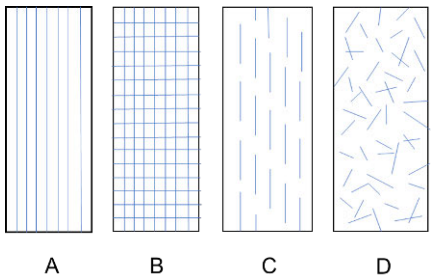

Figure 1. Orientation of fibers: (A) Unidirectional continuous and aligned fibers, (B) bidirectional continuous and aligned fibers, (C) Unidirectional discontinuous fibers, and (D) Random discontinuous fibers.

2.3.1 Fiber length

The length of the reinforcing fibers is critical in stress and load transfer from the polymer matrix to the reinforcing fibers. It is imperative that the length of the fiber must be equal to or greater than the critical fiber length to efficiently transfer stress between the fibers. Long fibers offer better mechanical properties than short glass fibers (Zhang et al., 2017). Fibers that are shorter than the critical fiber length behave like particulate fillers and do not effectively reinforce the composite, and may cause the matrix to deform around the fibers and produce little stress transfer, practically with no reinforcement (Garoushi et al., 2006). Long continuous fibers have the highest anisotropic mechanical properties. The reason is that the large surface area of fibers enables bonding of fibers to the polymer matrix to occur on a larger surface area. Discontinuous short FRC has properties that relate to the direction of fibers but also to the length of fibers (Garoushi et al., 2012). Generally, increasing the fillers' aspect ratio results in an increase in the modulus of elasticity of the composite (Jiang et al., 2007). The influence of the dimensionality (1D, 2D, and 3D), *i.e.*, the aspect ratio, of the fiber is pronounced in the tensile properties (Pradhan et al., 2013). The effect of fiber length on ultimate strength of a material is schematically represented in Figure 2.

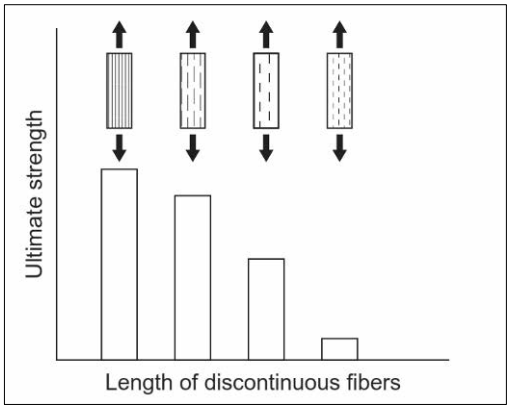

Figure 2. Effect of the length of oriented fibers on the ultimate strength of FRC; adopted from (Vallittu and Matinlinna, 2017).

2.3.2 Fiber quantity

Quantity of fibers in a matrix system is estimated by weight percent (Wt.-%) or by volume percent (Vol.-%). However, the investigators generally recommend estimation by Vol.-% due to the differences in the density of different fibers (Kumar et al., 2016). In structural FRC composites, volume fraction of fiber is roughly about 60 Vol.-%. Meanwhile, in dental related FRC materials, the volume fraction of fiber

is relatively low as the glass fibers have to be covered with an unfilled polymer layer (Vallittu, 2015; Abdulmajeed et al., 2011).

Strength and modulus of elasticity of a material are vital properties in prosthodontic applications. Higher stiffness is necessary for fiber-reinforced FPD frameworks because they must support the more brittle overlying restorative composite. Through "rule of mixtures", the properties of a composite material can be estimated. Although, a greater Vol. fraction of fibers enhances the strength and stiffness of the composite material, as expected from the rule of mixtures. However, the maximum volume fraction is about (80%) beyond which fibers can no longer be surrounded by the matrix. According to rule of mixtures, properties such as density, coefficient of thermal expansion, elastic modulus, shear modulus, tensile strength *etc.*, can be estimated (Kim et al., 2001).

2.3.3 Fiber distribution

The distribution of fibers in a resin matrix system is crucial and fundamental in deciding the mechanical properties of that material (Khan et al., 2015). Evenly distributed fibers have a beneficial effect on fatigue resistance. That said, more cyclic stresses would be borne by the material. Agglomeration and clustering of fibers in one place may have a negative effect on the fracture toughness, flexural strength, and compressive strength of a material. Similarly, the uniformity, regularity and location of the fiber-rich part of the sample significantly influences the strength. If samples with the same geometry and dimensions have variation in their fiber location, the strength of the specimen varies as well. The fibers have the highest reinforcing effect when they are located at the side of highest tensile stress in the sample (Narva et al., 2005b)

2.3.4 Fiber adhesion to polymer matrix

In order to warrant effective matrix-fiber stress transfer, bonding between fibers and matrix is crucial. There are a variety of interactions that control the load transfer between fibers and their matrices including chemical bonds, secondary interaction forces (van der Waals, acid/base) and mechanical interlocking. Although glass is chemically inert and the adhesion between glass fiber and resin is not evident (Vallittu, 1996). However, through silanization reliable chemical bonding between glass fibers and resin matrix can be attained (Liu et al., 2001). Silanes have bifunctional molecules; hence, they exhibit dual reactivity. At one end, the organic functional group copolymerizes with the resin matrix (Vallittu, 1997a). At the other end, the alkoxy group reacts with hydroxy groups present in glass and silica fibers to form a polysiloxane network (Si-O-Si) (Matinlinna et al., 2004).

Adhesion of reinforcing fibers other than glass fibers to the polymer matrix is based on different mechanisms. Adhesion of glass fibers is more physicochemical in nature whereas fibers of ultra-high molecular weight polyethylene (UHMWPE) can only be adhered after the fiber surface has been treated with high-energy plasma treatment for generating free radicals on the UHMWPE surface. Surface oxidation and etching treatment can be helpful in enhancing the aramid/kevlar-polymer bonding (Kalantar and Drzal, 1990). Whereas, chemical functionalization can effectively enhance the bonding ability of carbon/graphene to polymer matrix (Xu and Gao, 2015). Surface plasma treatment of UHMWPE fibers has the limitation of free radicals that limit active functioning time and therefore even plasma treated UHMWP fibers do not provide reliable bonding between the polymer matrix and fibers (Vallittu, 1997b; Alander et al., 2004).

2.3.5 Fiber diameter

Fiber diameter is an important parameter that has an effect on the mechanical properties of FRCs by having an impact on the aspect ratio of fibers. A study by Obukuro *et al.* suggests that flexural properties of an E-glass/UDMA-TEGDMA composite were affected by the fiber diameter. FRC with continuous unidirectional fibers and a diameter ranging from 20–30 μm were found to have highest flexural strength (Obukuro et al., 2008).

The number of individual fibers in the FRC can be increased by selecting fibers with a small diameter. The strength of a single glass fiber depends on its diameter. A larger diameter can be the reason for the reduction of strength. Typically used fiber diameters are 6–18 μm in diameter.

2.3.6 Fiber composition and type

Several reinforcing materials are available for FRC. Among them carbon/graphite, various glass, aramid and polyethylene are significant and commonly tested in dentistry (Ellakwa et al., 2002b). The mechanical properties of the resultant materials are affected by the unique geometry of each type of the fiber used (Ellakwa et al., 2002b). An overview of some commonly used pre-impregnated FRCs and FRCs that require impregnation is presented in Table 1.

Table 1. Examples of some pre-impregnated FRC products, FRC products that need impregnation and their use in dentistry.

Product	Manufacturer	Fiber type	Fiber orientation	Applicability in dentistry
Pre-impregnated products				
everStick	Sticktech Ltd., Turku, Finland	E-glass	Continuous unidirectional	For minimally invasive fiber-reinforced composite bridges, post and core structures, splinting, orthodontic retainer
Fibrekor	Pentron Clinical Technologies, Wallingford, CT, USA	S-glass	Continuous unidirectional	Post for the reinforcement of an endodontically involved tooth
Splint-It	Pentron Clinical Technologies, Wallingford, CT, USA	S-glass	Continuous braided	Splinting
Splint-It	Pentron Clinical Technologies, Wallingford, CT, USA	S-glass	Continuous woven	Splinting
Splint-It	Pentron Clinical Technologies, Wallingford, CT, USA	S-glass	Continuous unidirectional	Splinting
Vectris frame and single	Ivoclar Vivadent, Schaan, Liechtenstein	Glass	Continuous unidirectional / woven	Frameworks for anterior and posterior crowns
C-Post	Bisco	Carbon	Continuous unidirectional	Post for the reinforcement of an endodontically involved tooth
EverX Posterior	GC Corporation	Glass	Discontinuous random	Restoring the posterior cavities
EverX Flow	GC Corporation	Glass	Discontinuous random	Core build-up, direct restorations
Nulite F	Nulite Systems International, Hornsby, Australia	Glass	Discontinuous random	Posterior restoration
Alert	Jeneric/Pentron, Wallingford, CT, USA	Glass	Discontinuous random	Posterior restoration
Products need impregnation				
Connect	Kerr Corporation, CA, USA	UHMWP	Continuous braided	Frameworks for anterior and posterior crowns
Ribbond	Ribbond, Seattle, WA, USA	polyethylene	Continuous braided	Splinting, restoration, orthodontic retainer

2.3.6.1 Glass fibers

Glass fibers are widely used and the most popular reinforcing-fibers in FRC because of their transparent appearance with high tensile strength and low extensibility (Mangoush et al., 2017). Their favorable mechanical properties such as excellent impact and compressive strength, high modulus of elasticity and flexural strength make them a popular choice as reinforcing agent. Though several types of glass fibers are available, the most durable, ease of silanization and adhesion to resin matrix are E-glass (E=electric) fibers. E-glass contains calcium-alumino-borosilicate. It has high strength and stiffness but low impact and fracture resistance (Barbucci, 2002). On the contrary, S-glass fibers (S=strength) are high strength glass fibers (Barbucci, 2002). Although, S-glass fibers offer the highest tensile strength among all glass fibers, their high processing cost make them less attractive in high volume industrial applications. S-glass is mostly used in the aerospace industry. S-glass is divided into subclasses (S2, S3 etc.) based on the surface sizing of the fibers. R-glass (R=chemically resistant) is a less common glass fiber used as a reinforcing agent (Dyer et al., 2004). R-glass contains alumino silicate glass without MgO and CaO, is used when high mechanical requirements are desired for reinforcement. This glass also has increased strength and acid corrosion resistance. Different types of glasses with their chemical composition and properties are described in Table 2.

Table 2. Chemical composition and properties of commonly used glass fibers (modified from Avci et al., 2019).

Glass	Chemical composition (Wt.%)					Tensile strength (GPa)	Modulus (GPa)	Prominent feature
	SiO_2	Al_2O_3	CaO	MgO	B_2O_3			
E	53–55	14–16	20–24	20–24	6–9	3.4	72.3	↑ strength & electric resistance
A	70–72	0–2.5	5–9	1–4	0.5	3.3	68.9	low strength
R	60	25	6–9	6–9	-	4.1	85.5	strength & acid resistance
S	62–65	20–25	-	10–15	0–1.2	4.9	86.9	↑ tensile strength

The other less common glasses available are: A-glass used as filler for plastics with limited chemical resistance to water and C-glass also called chemical resistant glass. Glass fibers vary also in their radio-opacity, which is an important material property for dental resin composites. High radio-opacity is desired for visibility of the material in X-rays but in cone-beam X-rays, high radio-opacity may cause artefacts in the images (Kuusisto et al., 2015).

2.3.6.2 Ultra high molecular weight polyethylene (UHMWPE) fibers

UHMWPE fibers are biocompatible and thermoplastic with a relatively low modulus of elasticity, a density of 0.94 g/cm3 and good impact strength. These fibers are made of aligned polymer chains. Their white color makes them suitable for use in esthetic dental applications (Edwards, 1998). The previous studies equating the mechanical properties of different reinforcing fibers have indicated that the impact strength of UHMWPE fiber in composites is 20 times greater than that fiber of glass, aramid and carbon (Barbucci, 2002; Ellakwa et al., 2002b).

Despite encouraging and supporting properties, UHMWPE fibers have some shortcomings also. These include inadequate tensile strength and elastic modulus, high creep, low melting point (about 147°C), and above all low surface energy which makes adhesion between fiber and matrix unsatisfactory (Gutteridge, 1992; Bae et al., 2001). UHMWPE fibers are chemically too inert, having almost no reactive groups, resulting in weak interfacial bonding and poor compatibility between the fiber and the polymer resin (Vallittu, 1997b; Narva et al., 2005b; Narva et al., 2005a). Hence, most of the surface treatment methods are not practical.

2.3.6.3 Aramid/Kevlar fibers

Aramid (also known as kevlar) fibers are synthetic fibers derived from aromatic polyamides. The fibers offer outstanding strength, flexibility, low density and abrasion tolerance (Murphy, 1998). Studies have shown that using aramid fibers significantly improve flexural strength of PMMA (Vallittu and Lassila, 1992; Uzun et al., 1999) and composite resin (Ellakwa et al., 2002a; Uzun and Keyf, 2003). However, the compressive strength of these fibers is poor hence, they are recommended in combination with other reinforcing agents in order to attain adequate compressive strength (Barbucci, 2002). When these fibers are subjected to bending or axial compression, they go into non-linear plastic deformation. These fibers exhibit a yield point at a compressive strain of 0.3–0.5%. A structural defect known called “Kink bands” forms at 45–60^{o} to the fiber axis. Due to compressive buckling of the aramid molecules by molecular rotation of the amide carbon-nitrogen bond, which in turn reflects weak lateral properties of this highly anisotroic material (Jassal and Ghosh, 2002). Though other favorable features such as thermal and chemical stability, high glass transitional temperature and excellent hardness of fibers are present, poor bonding with resin matrix, make these fibers unsuitable as reinforcing agent. Furthermore, the bright yellow golden color of these fibers also has a negative effect on appearance of restoration and can limit their use in esthetically demanding situations (Barbucci, 2002).

2.3.6.4 Carbon/Graphite fibers

Due to some favorable properties such as biocompatibility, stiffness, high compressive and tensile strength, low density, high fatigue strength, and elastic modulus, the use of carbon/graphite fibers is immense (Khan et al., 2017b). In dental applications, initially carbon fibers have been used to reinforce removable dentures, restorative composite filling, implant and implant-supported prostheses, and interim fixed partial dentures (Vallittu, 1996; Yazdanie and Mahood, 1985; Larson et al., 1991). The size of a carbon fiber is usually around 5 to10 μm in diameter and mainly composed of carbon atoms that are bonded together in crystals and aligned parallel to the long axis of the fiber. This crystal alignment gives the fiber a high strength-to-volume ratio (Varley et al., 2019). However, their clinical use is now restricted to prefabricated endodontic posts. Their black color limits their use in esthetically demanding applications.

The mechanical properties of carbon fiber vary over a large range depending on the temperature of the final heat treatment. There are two general categories of carbon fiber produced depending on the final temperature: high-modulus or high-strength. In terms of final mechanical properties, carbon fibers can be roughly classified into ultra-high modulus (>500 GPa), high modulus (>300 GPa), intermediate modulus (>200 GPa), low modulus (100 GPa), and high strength (>4 GPa) carbon fibers (Huang, 2009).

2.3.6.5 Other fibers

Recently, nylon fibers are gaining attention and interest because of their shock and stress resisting features. However, water sorption has a deleterious effect on the mechanical properties of these fibers. Though fracture toughness of PMMA can be increased using nylon fibers, glass and aramid fibers have demonstrated higher levels of fracture toughness compared to nylon fibers in PMMA (John et al., 2001). Polyester fibers have also been suggested to reinforce PMMA dentures. Though these fibers improve impact strength, no effect on flexural strength and surface hardness was reported (Chen et al., 2001). In addition, rigid rod polymers have also been employed in many applications such as fillers in composite materials, denture base polymer, and bridge material (Vuorinen et al., 2011a). Rigid rod polymers have molecular chains with restricted chain movement, with overall good mechanical properties e.g., polyphenylenes (Vuorinen et al., 2008; Vuorinen et al., 2011b). The detailed fiber classification is schematically presented in Figure 3.

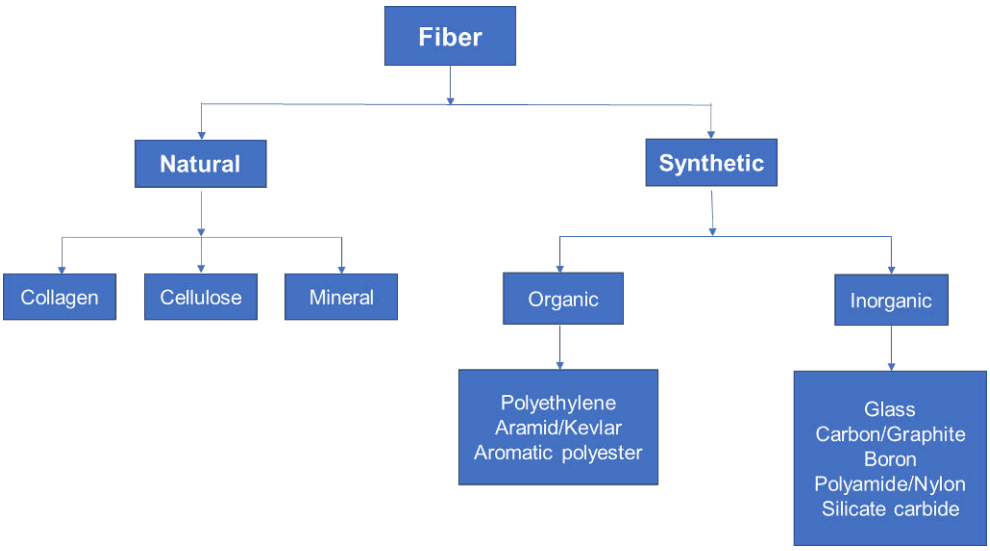

Figure 3. Classification of fibers used in reinforcing a material.

2.4 Resin matrix system of FRC

A variety of resin matrix systems have been proposed to impregnate and bind reinforcing fibers. In general, resin matrix systems of FRC are classified broadly into either linear thermoplastic matrix or cross-linked thermoset matrix. Thermoplastics also known as thermo softening matrices are polymers that soften during heating and harden upon cooling. While thermosetting polymers cure either by chemical reaction or heat application, and their cure is irreversible.

Different polymer matrices have been experimented on for a workable thermoplastic such as poly(ethylene terephthalateglycol) (Goldberg et al., 1994; Jancar and Dibenedetto, 1993), polycarbonate (Goldberg et al., 1994; Jancar and Dibenedetto, 1993), Poly(1,4-cyclohexylene dimetylene terephtalate glycol), polyurethane (Goldberg et al., 1994), nylon-6 (Goldberg et al., 1994), nylon-12 (Goldberg et al., 1994) and polypropylene (Jancar and Dibenedetto, 1993). Similarly, thermosetting polymers such as (*bis*GMA/PEGDMA) and (*bis*GMA/TEGDMA) copolymers have also been tested (Karmaker et al., 1997). However, these polymers failed mainly because of bonding properties to veneering particulate resin composite and also due to their handling properties. Despite the limitations of bonding characteristics of thermoset FRCs of dimethacrylate and epoxy polymer matrix, they are widely desired polymers in dental fiber-reinforced composites. However, a special group of polymer formulation comprising both linear and cross-linked systems together, which do not merge by chemical reaction but by interpenetration

have been suggested for FRC use. These are called semi-interpenetrating polymer network (semi-IPN) (Vallittu, 1995b; Goldberg et al., 1994).

2.4.1 Thermoplastic polymers

Thermoplastic polymers are easily molded and shaped under heating. These polymers are typically hard/brittle at room temperature. However, they become soft/flexible upon heating. The temperature at which this transition occurs is called glass transition temperature (Tg). Above its Tg and below its melting point, the physical properties of a thermoplastic change drastically without an associated phase change. Thermoplastics may have a high molecular weight. The polymeric chains are associated with intermolecular forces, which weaken rapidly on heating, yielding a viscous liquid. Thermoplastic polymers can be linear or branched chain. These polymers are used to produce parts by various polymer processing techniques such as injection molding, compression molding, and extrusion (Vivaldo-Lima and Saldívar-Guerra, 2013). Examples include: low density polyethylene and high density polyethylene, PMMA, polypropylene, poly(vinyl chloride) and polystyrene. Bonding of thermoplastic polymer matrix to reinforcing fibers is based on physical adhesion only, whereas thermosets may also involve chemical adhesion.

2.4.2 Thermosetting polymers

Unlike thermoplastic, thermosetting polymers form irreversible chemical bonds during the curing process. The constituent polymers cross-link during the polymerization process to form an unbreakable bond, hence thermosets do not melt or reshape even at elevated temperatures. Unlike thermoplastic pellets, the components of thermoset polymers are stored in liquid form, usually in large tanks or containers. These are cross-linked polymers and cannot be reused (Mccabe and Wilson, 1974). Examples include bakelite, epoxy resins, polyurethanes and poly(*bis*GMA). Thermoset resins may bond with reinforcing fibers chemically if appropriate surface sizing of fibers has been made. For instance, glass fiber surface can be silanized with silanes containing similar chemical reactive group, as in the thermoset resin, and by polymerization of the resin, covalent bonding between resin and fiber would take place (Thomason, 2019)

2.4.3 Semi-interpenetrating polymer network (semi-IPN)

By definition, IPN is a polymer network with one or more networks having one or more linear or cross-linked polymers that are interlaced on a molecular scale. In semi-IPN FRCs, methacrylate-based resins are the resins employed to impregnate

fibers of the FRCs. For linear polymer parts of the semi-IPN, PMMA is commonly used, which is a denture base resin also (Segerström et al., 2005; Ruyter and Svendsen, 1980; Ruyter, 1982). In the case of using PMMA in denture bases, MMA is typically mixed with pre-polymerized powder beads of PMMA. The MMA monomer dissolves the PMMA beads. A minor proportion of the cross-linking monomer system is also included, such as ethyleneglycol dimethacrylate (EGDMA), in denture base linear PMMA polymer to improve mechanical properties (Vallittu and Özcan, 2017). After initiation of the free radical polymerization of MMA monomers, the linear polymer chains are bound by cohesive forces of van der Waals (also known as London forces) (Vallittu and Özcan, 2017). At the same time, the polymerized PMMA network is entrapped to the surface of PMMA beads by the IPN system. A similar kind of IPN is used in dental FRCs: PMMA containing matrix of linear PMMA and cross-linked multifunctional co-monomers (e.g. *bis*GMA, urethane dimethacrylate (UDMA) or TEGDMA) is used to bind the fibers. The linear polymer part of PMMA of the polymer matrix is dissolvable and can be used for adhering new resin to the surface of FRC with a second IPN, which is called secondary IPN referring to the bonding interface. Figure 4 depicts the structure of linear and cross-linked polymers and the IPN system.

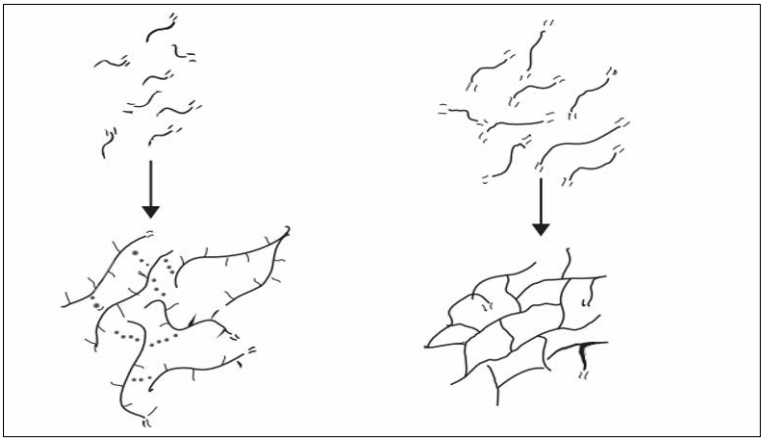

Figure 4. Monofunctional monomer (e.g., MMA) produced linear polymer (on the left) whereas bifunctional monomers (e.g., *bis*GMA) produce cross-linked polymer (on the right). By combining these two kinds of polymers, the IPN system is formed. Adopted from Vallittu and Matinlinna, 2017).

The rationale behind using secondary-IPN is to form a durable bond with laboratory (indirect) FRC restorations or repairs. In directly made restorations, adhesion of the veneering resin composite or resin luting material to the surface of the FRC substructure can be based on free radical polymerization of the veneering composite

to the resin matrix part of the FRC because of the oxygen-inhibited layer present on the substrate surface. However, there is no oxygen inhibition layer present in the indirectly made restorations. On the other hand, semi-IPN FRC contains a linear polymer along with cross-linked polymer. The adhesion of the resin luting material can be achieved by diffusion of the monomers of the resin luting material into the polymeric matrix of FRC, forming the secondary-IPN bonding layer (Lastumäki et al., 2003; Vallittu, 2009) (Figure 5).

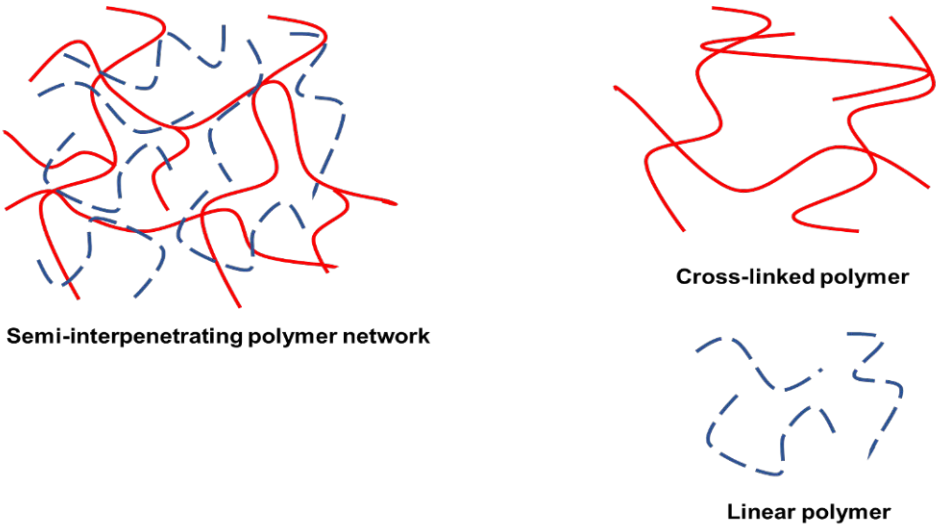

Figure 5. Schematic representation of semi-interpenetrating polymer network (semi-IPN) structure, cross-linked and linear polymers.

2.5 Fabrication of dental fiber-reinforced composites

FRCs are fabricated by blending the reinforcing fibers (continuous or discontinuous), resin matrix and additives together. This blending process of the constituents may be processed before or during the shaping (Akovali, 2001). The constituents blended before the shaping process, is called the compound construction stage. During this stage, the constituents are blended into a preliminary form that is suitable for shaping the FRC final product. In this stage, the FRC is in an uncured state and can be delivered either in molding compound form or in pre-impregnated compound form, also called prepreg. Prepregs are handled into the preferred shape during the tooling stage of the final fabrication process. Most resin-based composites for dental use are delivered to the end-user as molding compound or prepreg. In dental FRCs, the prepreg is made of uncured dimethacrylates with PMMA and the final shaping and curing are executed by the clinician. In many technical fields,

prepregs are fabricated by the hot melt method and the solvent impregnation method (Rosato and Rosato, 2004). In hot melt method, viscosity of the resin is reduced by heat under pressure for a short time during impregnation of the fiber reinforcement. Whereas the viscosity of the resin is reduced by adding solvent in the solvent impregnation method.

In contrast, for the shaping process, the constituents are blended and their final shape is given and cured into their final shape as an end-product. An example of this include FRC root canal posts.

2.5.1 Impregnation of fibers

The optimal fiber-reinforcing effect depends on intimate contact of reinforcing fibers to the resin matrix. Infiltration of resin matrix between the spaces of the fibers is termed resin impregnation. Efficient impregnation contributes to a successful interfacial adhesion. With efficient impregnation, stresses and loads are transferred adequately from the material to its reinforcing fibers. On the contrary, deficient or incomplete wetting can instigate and provoke void formation and premature failure (Ruyter et al., 1986; Vallittu, 1994; Vallittu, 1995a; Vallittu, 1995b).

Successful resin impregnation depends upon viscosity of the resin matrix, wetting properties of fibers, distance between individual fibers in matrix system and fiber orientation (Ruyter and Björk, 1986).

Impregnation of the fibers can either be performed by hand or through a specific pre-impregnation manufacturing process (Goldberg and Burstone, 1992). The hand method is considered adequate provided that the impregnation is desired with a low viscosity resin system. However, for viscous resins, a specific pre-impregnation manufacturing process is recommended. Viscous resin (e.g. *bis*GMA) may not wet the fibers adequately using the hand method.

Several manufacturing techniques have been suggested to boost the impregnation of resins between the fibers. Most of the suggested techniques are associated in forming a FRC prepreg. For highly viscous denture base acrylic system, an explicit prepreg method was developed by Prof. Pekka Vallittu in which PMMA with a molecular mass of 220,000 broke down in an extremely evaporative solvent and the fibers became saturated with the PMMA-based solvent (Vallittu, 1999). Accelerated evaporation of the solvent makes the PMMA polymer highly porous between the fibers. When monomer liquid is introduced, fibers of the prepreg are wetted and react with the porous PMMA between the fibers.

For impregnation of fibers with thermoset polymers, viscosity of the monomer system has an important role. In contrast to PMMA containing dental acrylate systems, thermoset polymers have no powder bead in the resin. Therefore, the fibers are in close contact with each other. Due to high fiber loading in these systems, space

for the resin between the fibers is less (Kolbeck et al., 2002). For optimizing the degree of impregnation, fiber loading and allowing formation of an IPN system for the polymer matrix of FRC, PMMA beads are first dissolved into polymer chains which are then mixed with the co-monomer system of dimethacrylates. This process is used in the products by Stick Tech-GC Group.

2.6 Interfacial adhesion between FRC and resin luting material

FRCs are mainly used as a bonding substrate that is cemented with different materials. Apart from the interfacial region between the resin matrix and reinforcing fibers, the adhesive interface between different resin luting materials and FRC substrate is equally influential. The affinity between the resin matrices of the adherent and adherend is essential to attain an effective adhesion (Clyne and Hull, 2019). As a whole, the crucial aspect in attaining the improved mechanical properties in FRC applications is the ability of the constituents (fibers, matrix and veneering materials) to be effectively adhered together (Vallittu, 2001).

Adhesion between FRC and resin luting material occurs by several mechanisms such as physical interlocking or chemical adhesion. Physical interlocking between FRC and the resin luting material is influenced by the surface topography of the fibers present in FRC. However, this type of bonding may not be adequate to withstand higher loading (Kim and Mai, 1998). While chemical bonding is created due to covalent bond formation between the constituents of FRC and the resin luting material. Parameters such as fiber topography, number of covalent bonds and matrix type greatly influence the strength of chemical bonding (Kim and Mai, 1998; Vallittu, 1997a; Debnath et al., 2003).

In contrast, diffusion of monomers from one surface (resin luting material) into the molecular network of the other surface (FRC) forms a bond. The durability of this bond is governed by the amount of monomer diffusion and the number of molecular chains involved (Kim and Mai, 1998). The higher the monomer diffusion, the higher would be the degree of interdiffusion. However, the dissolving gradient of the monomer is governed by the solubility parameters, monomer interaction time with the FRC substrate, room temperature monomer interacted with the FRC, shelf-life and polymeric content of semi-IPN based FRC structures (ChenLee and Ho, 1998). The example of an interdiffusion mechanism is the use of semi-IPN system.

3 Aims of the thesis

The series of studies of the thesis primarily focused on determining the nanomechanical properties of the adhesive interface between resin luting material and FRC. Special emphasis was set on the dissolving capability of the monomers of the adhesive/primer and solidification of the dissolved PMMA enriched surface layer of the semi-IPN based FRC. The specific aims and hypotheses were:

1. to characterize nanomechanical, chemical and thermal properties of the secondary-IPN layer of the FRC prepregs that had been stored for up to two years before curing. The nanohardness and modulus of elasticity of semi-IPN polymer matrix were examined at various depths of the FRC substrate. The working hypothesis was that the PMMA gradient would be lower due to aging of FRC prepregs (**Study I**).
2. to evaluate the secondary-IPN layer of the semi-IPN polymer matrix FRC that had been stored for up to three years before curing. The nanohardness and chemical properties of the secondary-IPN layer were examined, and was hypothesized that the properties would be affected due to the aging of the FRC prepregs and the use of different adhesive/primers (**Study II**).
3. to determine the influence of different monomer systems on the tensile bond strength (TBS) between FRC and resin luting material, also the effect of the monomer systems on FRC made of prepregs aged for different intervals before use. It was hypothesized that the monomer systems of adhesive/primers and resin luting material would affect TBS between the FRC and resin luting material (**Study III**).
4. to investigate the TBS between a polymerized semi-IPN FRC with an intact or ground surface and a resin luting cement using adhesives/primers for different lengths of time. The hypothesis was that the PMMA gradient of the FRC intact is similar to that of the FRC ground, and hence there would be no effect on TBS (**Study IV**).

4 Materials and Methods

The materials used to fabricate semi-IPN based FRC samples in studies I–IV are listed in Table 2.

Table 2. Materials used in studies I–IV

Material	Manufacturer	Composition	Study
everStick C&B	StickTech – GC, Turku, Finland	Bisphenol A-glycidyl methacrylate, poly(methyl methacrylate), substituted methacrylate (<0.5%), hydroquinone (<0.5%) photoinitiator system	I, II, III, IV
Rapid Repair	DeguDent GmbH, Hanau, Germany	Poly(methyl methacrylate) 95–100% methyl methacrylate (80-100%), ethylene dimethacrylate (1–20%), N,N-dimethyl-p-toluidine (1%–< 3%)	I
StickRESIN	GC, Tokyo, Japan	(1-methylethylidene)bis[4,1-phenyleneoxy(2-hydroxy-3,1-propanediyl)] bismethacrylate (25–50%), 2,2'-ethylenedioxydiethyl dimethacrylate 25–50%, 2-dimethylaminoethyl methacrylate (0.1–0.5%), photoinitiator system	II, III, IV
Composite Primer	GC, Tokyo, Japan	2-hydroxyethyl methacrylate (30–60%), tetrahydrofurfuryl methacrylate (10–30%), urethane dimethacrylate (10–30%), photoinitiator system	II, III
G-Multi PRIMER	GC, Tokyo, Japan	Ethyl alcohol (90–100%), phosphoric acid ester monomer (1–5%), dimethacrylate component (1–5%)	II, III, IV
G-Cem LinkAce	GC, Tokyo, Japan	Urethane dimethacrylate (25–50%), dimethacrylate (5–10%), phosphoric acid ester monomer (1–5%), dual-curing initiator system	II, III, IV
Tetrahydrofuran (THF)	CDH laboratory chemicals, New Delhi, India	Tetrahydrofuran (>99%)	II
Eco-Cryl Cold	Protechno	PMMA (95-100%), MMA (80–100%), ethylene dimethacrylate (1–20%), N,N-dimethyl-p-toluidine (1–2%)	III

4.1 Study I

4.1.1 Fabrication of bar-shaped FRC samples

A semi-IPN based FRC (everStick C&B, StickTech-GC, Turku, Finland) prepreg was selected and stored at 4°C for various lengths of time, *i.e.*, two-weeks (fresh), 6-months, and 2-years. For each storage group, 10 mm of the FRC material was cut off from the fiber frame. Next, the prepreg was polymerized for 5 min in a light curing oven (Labolight LV-III, GC Corporation, Tokyo, Japan) followed by additional 15 min curing in a vacuum oven (Espe Visio® Beta Vario, Espe, Seefeld, Germany) to eliminate an oxygen inhibited surface layer (Figure 6).

A self-curing acrylic resin (Rapid Repair, DeguDent GmbH, Hanau, Germany) was used to embed the FRC samples for analysis. The acrylic resin was decanted into a tissue-processing cassette; the resin was filled up to 2 mm above the extended sidewalls of the cassette for ease of FRC slicing. Subsequently, a 10 mm polymerized FRC bar was introduced with its length along the horizontal axis in the acrylic matrix in such a way that half of the diameter (approximately 0.85 mm) of the stick was embedded inside the acrylic resin and the remaining half was free from any contact. A single FRC bar was centered in each resin-filled cassette during the sticky stage of polymerization (Figure 7). Five samples were prepared for each group *i.e.*, two weeks (fresh-group), 6-months, and 2-years samples (prepared with FRC manufactured 2 years before making the samples). The cured FRC samples were stored in a desiccator for 48 h before any further process or analysis were undertaken.

Figure 6. Bar shaped polymerized FRC.

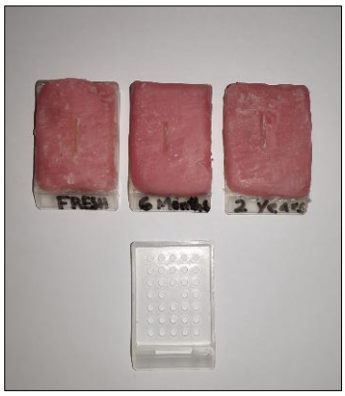

Figure 7. Tissue-processing cassettes filled with self-cured PMMA and embedded bar shaped FRC.

4.1.2 Mechanical testing

Nanoindentations of the polymer matrix phase of the FRC were obtained with a nano-mechanical tester (Bruker, Santa Barbara, CA, USA) with loading and unloading rates of 0.05 mN/s and a 10 s dwell time. The maximal load was set to 0.5 mN (Fig. 2). Initially, each FRC bar was sectioned 200 µm longitudinally along its long axis with a microtome saw (SLEE CUT 5062, SLEE Medical, Mainz, Germany) to provide a smooth and even surface for nanoindentation of the polymer matrix (Figure 8). During testing, the indenter (three-sided pyramidal Berkovich diamond tip, 100 nm radius) was pressed randomly onto the sample's polymer matrix surface (between the fibers) (Figure 9). On each sample, 5 indents were made at least 50 µm apart to avoid overlapping of the indentations. The nanoindentations being introduced on the top surface of each sample from the tested groups comprised "stage 1." Next, with a microtome saw, a 100 µm slice was cut longitudinally and evaluated for 5 nanoindents. This stage of evaluation was named "stage 2". The nanoindentation evaluation of "stage 3" was performed by cutting 100 µm off once again. To evaluate the nanomechanical properties (nanohardness and modulus of elasticity) of the polymer matrix, 4 slices (100 µm each) were cut from stage 1 to stage 5 (Figure 10).

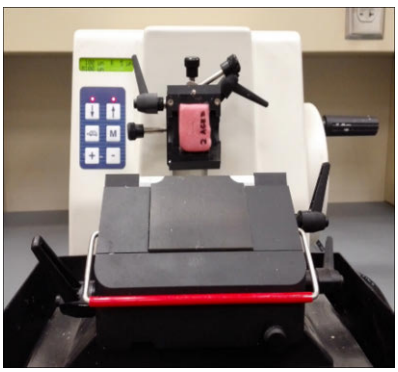

Figure 8. Longitudinal slicing of bar shaped FRC with a microtome saw.

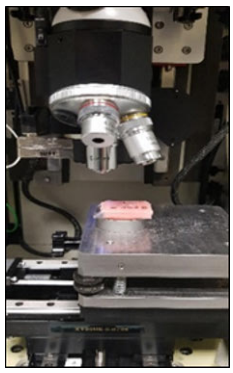

Figure 9. Nanohardness evaluation test.

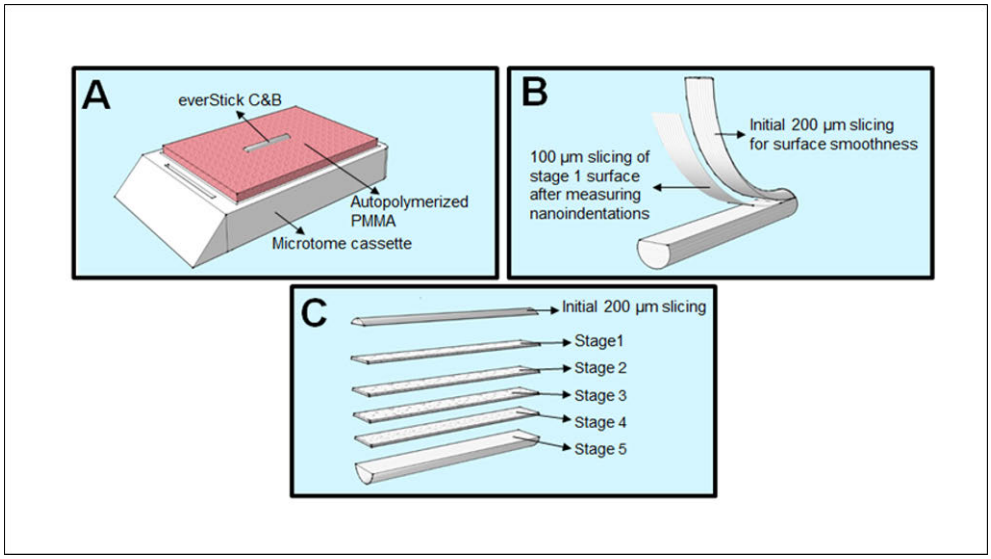

Figure 10. Sample preparation for nanomechanical testing: (A) 10-mm-long cured FRC sample partially embedded in autpolymerized acrylic resin, (B) Initial 200 µm slicing of the FRC for smoothing of the tested stage 1 surface, (C) Subsequent longitudinal slicing of 100 µm each from stage 1 to stage 5 for nanomechanical and chemical analysis. Adopted from original publication I.

4.1.3 Chemical testing

Raman spectra of the top (stage 1) and the core (stage 5) surfaces were acquired using a ProRaman-L Analyzer (TSI®, Shoreview, MN, USA) with an excitation laser beam wavelength of 785 nm. The scanning was undertaken between 250 and 2350 cm^{-1}. However, special emphasis was made with the scanning at 1450 cm-1 and 1640 cm^{-1} to evaluate the structural fingerprints of PMMA and *bis*GMA, respectively. Similarly, X-ray diffraction (XRD) patterns of stage 1 and stage 5 surfaces were determined using a D-8 Discover X-ray diffractometer (Bruker,

Karlsruhe, Germany) in the 2θ range of 30–90°, at a scan speed of 2°/min with an increment of 0.02 in locked coupled mode.

4.1.4 Thermal testing

Thermogravimetric analysis (TGA) and differential scanning calorimetry (DSC) were estimated using SDT Q600 (TA Instruments, New Castle, DE, USA). The glass-transition temperature (Tg) of stage 1 and stage 5 of the FRC surfaces was estimated separately. For thermal analysis, individual samples (approximately ⌀ 1.7 mm, L= 5 mm, and weight in the range of 5.80–6.26 mg) were placed in an alumina pan inside the heating compartment, and then the sample was heated at 10°C/min from 23°C to 600°C under a nitrogen environment. The acquired data were evaluated through proprietary software.

4.2 Study II

4.2.1 Fabrication of FRC samples

A semi-IPN based FRC (everStick C&B, StickTech-GC, Turku, Finland) prepreg was selected and stored at 4ºC for various lengths of time, *i.e.*, 1.0, 1.5, and 3.0 years. A silicone mold (Affinis Putty, Coltene Whaledent) was used to prepare and standardize the shapes and thicknesses of the samples. The FRC prepreg was cut off, placed inside the silicone mold, pressed against two glass plates to obtain a plane surface with a 0.7 mm width, and subsequently light-polymerized for 40 s with an irradiance of 1150 mW/cm^2 using Elipar S10 (3M ESPE, USA). Each aging group was further divided into four subgroups (n=6) according to the primer used to pre-treat the FRC surface: no pre-treatment, pre-treatment with a light-curing dimethacrylate adhesive primer (StickRESIN, GC, Leuven, Belgium), universal primer (G-Multi PRIMER, GC, Tokyo, Japan), and primer intended for composite substrates (Composite Primer, GC, Leuven, Belgium). A single coat of the primer for each subgroup was applied on the FRC. The samples were thereafter stored under a light-protection shield for 3 min to allow the monomers to penetrate the FRC surface. Subsequently, the specimens were light-polymerized for 20 s. A 0.3 mm thick resin luting material (G-CEM LinkAce, GC, Tokyo, Japan) was bonded on a pre-treated FRC surface. A Mylar sheet and a glass plate were used to achieve a smooth surface of resin luting material. The samples were subjected to a final light-polymerization for 40 s. They were thereafter polished with a 1200-grit silicon carbide paper under running water. Finally, twenty-four samples (n=24) of dimensions 4.5×3×1 mm^3 were prepared from each aging group (Figure 11).

Figure 11. Rectangular shaped polymerized FRC samples bonded with resin luting material.

4.2.2 Chemical analyses

The degree of monomer conversion (DC%) of the resin luting material was evaluated using Fourier-transform infrared spectroscopy (FTIR, PerkinElmer, Waltham, MA, USA) in the attenuated total reflectance (ATR) mode. As a control measurement for DC%, a sample of the resin luting material (LinkAce, GC) of thickness 0.3 mm was placed on the ATR sensor (ZnSe-crystal) to measure the DC% at the bottom. The upper surface of the specimen (n=6) was covered with a Mylar sheet and a glass slide of thickness 1 mm was pressed slightly against the ATR to establish a good contact with the specimen. The light source was placed in contact with the glass slide. The photo-polymerization was performed using a hand-held light-polymerizing unit for 40 s.

The experimental groups were prepared to evaluate the differences in the DC% compared with the control group and they were classified as follows: a. FRC without the application of primers on which a resin luting material (LinkAce, GC) was applied; b. FRC treated with StickRESIN followed by the application of the resin luting material; c. FRC treated with G-Multi PRIMER followed by the application of the resin luting material; d. FRC treated with Composite Primer® followed by the application of the resin luting material. The luting material side was always placed on the ATR sensor. The FRCs of the specimens of each group were photo-polymerized for 40 s; subsequently, the primer was applied and left on the surface of the FRCs for 5 s and immediately, the specimens were light-polymerized for 20 s, with the exception of the group where a primer was not used to treat the FRC surface. The treated FRCs were thereafter placed on top of the uncured luting cement and the DC% was measured before and after the photo-polymerization was performed. The DC% was calculated using the carbonyl C=O peak at 1716 cm^{-1} and normalized against the aliphatic C=C peak at 1638 cm^{-1}. The fraction of remaining double bonds was determined via a comparison of the maximum heights of peaks.

Raman spectra of the interface between the FRC and resin luting material were obtained using a computer-controlled laser Raman microscope, ProRaman-L Analyzer (TSI®, Shoreview, MN, USA) with an excitation laser beam wavelength of 785 nm. Specimens were placed on the computerized XYZ stage and a laser beam was focused at the adhesive interface layer near the interface area under a

magnification of 50×. The scanning was performed between 250 and 2350 cm^{-1} and the acquisition time for each spectrum was set to 10 s. Three measurements were obtained with different specimens from each group to confirm the reproducibility of the results.

4.2.3 Nanomechanical analyses

Nanoindentation was used to measure the nanohardness and modulus of elasticity at the FRC–resin luting material interface, *i.e.*, the surface where the adhesive interface layer formed. A polyethylene mold with an inner diameter of 6.0 mm and height of 4.5 mm was filled with a self-adhesive resin cement, Multilink® Speed (Ivoclar Vivadent, Schaan, Liechtenstein), up to the brim to embed the FRC specimen in such a way that half of the width of the specimen, *i.e.*, 1.5 mm, remained embedded inside the resin luting material and the other half was free from any interaction with the resin luting material (Figure 12 & 13). Four indentations were made on each specimen at the adhesive interface layer (Figure, 13; n=6) with the aid of 20× objective lens for accuracy, using a nanomechanical tester (Bruker, Santa Barbara, CA, USA) equipped with a Berkovich diamond indenter tip of nominal radius ≈100 nm. Loading and unloading rates of 0.5 mN/s were used with a dwell time of 10 s. The maximal load was set to 5.0 mN.

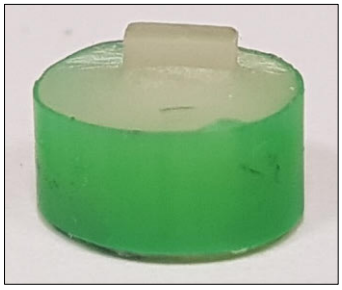

Figure 12. Study FRC sample embedded in resin luting material.

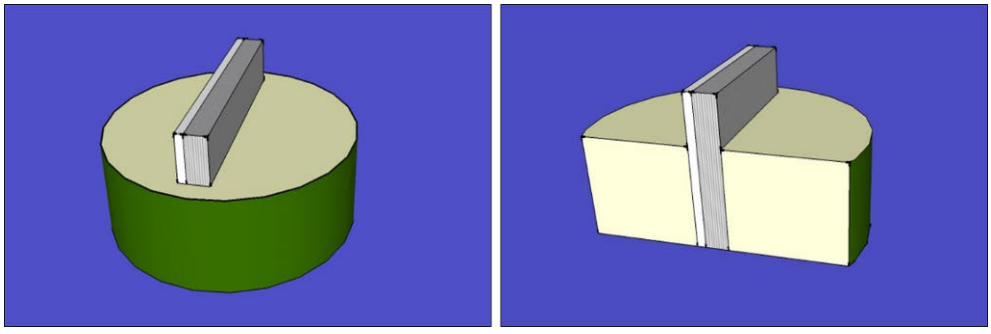

Figure 13. Schematic presentation of FRC sample preparation for nanoindentation testing.

4.2.4 Scanning electron microscopy (SEM) analysis

To demonstrate the presence of PMMA or poorly polymerized polymer phase at the adhesive interface area, the area was dissolved using solvent tetrahydrofuran (THF) (CDH laboratory chemicals, Delhi, India) for 30 s. SEM examination was conducted at 2 kV in a vacuum to eliminate chances of severe charging and image distortion problems using an SEM instrument (JEOL JSM 5900LV, Tokyo, Japan) to demonstrate the areas of the linear polymer structure with poor cross-linking density of polymer. The specimens from each group were analyzed at a magnification of 50× before and after the application of THF.

4.3 Study III

4.3.1 Fabrication of FRC samples

The methodology used in study III concurs partly with the methodology used in study II. The reader is advised to refer to section 4.2.1 to understand the initial steps of sample fabrication. Subsequently, each prepared sample was embedded in the middle of a silicone mold (9.0 mm × 3.0 mm × 4.5 mm), and a self-curing acrylic resin (Eco-Cryl Cold, Protechno; Vilamalla Girona, Spain) was filled into both sides of the sample. Afterwards, the sample was removed from the mold and stored in a desiccator for 24 h before further processing. For TBS testing, the sample blocks were sectioned with a precision diamond saw (IsoMet 5000, Buehler; Lake Bluff, IL, USA) at 1400 rpm under water cooling to the dimensions of 9.0 mm × 3.0 mm × 1.5 mm (Figure 14). The edges of each sectioned sample were finished with a 1200-grit silicon carbide paper under running water.

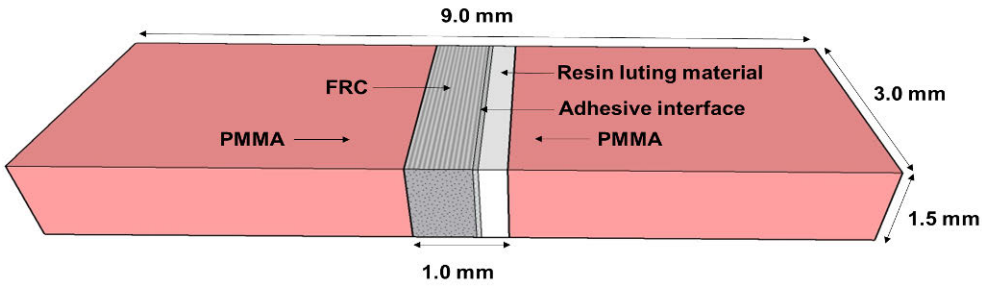

Figure 14. Dimensions of the tensile test sample. Adopted from original publication III.

4.3.2 Sorption test

A water sorption test was performed to stabilize the water content in the samples for bond strength testing. The thin, rectangular plate samples from each group were initially weighed (Mi). During the water sorption test, each sample was immersed in a glass vial containing 50 mL of distilled water and weighed at 1, 3, 7, and 14 d until the weight became stable (Mf). The water sorption values (Wsp, μg/mm^3) were calculated with the formula Wsp = (Mf-Mi)/V, using an analytical scale (Precisa, EP 320A; Dietikon, Switzerland) accurate to 0.1 mg.

4.3.3 Tensile bond strength (TBS) test

The tensile bond strength at the FRC–resin luting material interface, the location at which the adhesive interface layer was formed, was measured using a universal testing machine (Model no. 3369 Instron; Canton, MA, USA) under tension. The sample surface area was measured using a digital calliper (Mitutoyo, Tokyo, Japan). Each thin, rectangular plate sample was fixed to the grips of a tensile device with cyanoacrylate glue (Super Glue, Henkel/Loctite; Westlake, OH, USA) (Figure 15). The proprietary software of the testing machine recorded the failure loads in newtons and the bond strengths in megapascals. A load cell of 5 kN and a crosshead speed of 0.5 mm/min were used until fracture occurred.

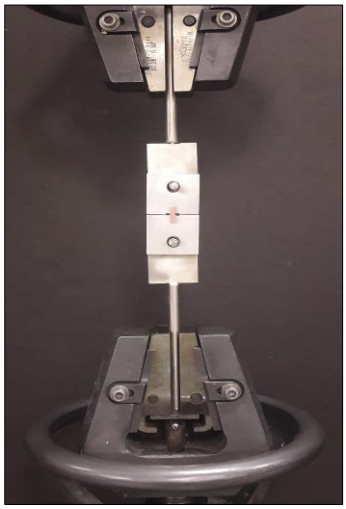

Figure 15. TBS sample mounted on a universal testing machine.

4.3.4 Fractographic analysis

Fractured plate samples were observed under a light microscope (Nikon SM2-10; Tokyo, Japan) at a magnification of 20×. The fracture type was defined by the

location of the fracture: within the FRC (cohesive), at the interface between the resin luting material and the FRC (adhesive), and with both the resin luting material and the FRC existing in the same fragment (mixed) (Khan et al., 2016; Khan et al., 2018c). The frequencies of different fracture modes were recorded for each group.

4.4 Study IV

4.4.1 Fabrication of FRC samples

A semi-IPN (based on bisphenol-A-glycidyl methacrylate (*bis*GMA) and poly(methyl methacrylate) (PMMA) FRC prepreg (everStick C&B, Stick Tech Ltd., GC Group, Turku, Finland) with dimensions 4×3×1 mm^3 was selected, photo-polymerized and divided in two categories: FRC intact (surface enriched with high-gradient PMMA) and FRC ground (the glass fibers and inner part of the polymer matrix are exposed). The FRC intact samples were prepared by light curing the FRC while pressing it between two glass plates. The light curing was performed using a hand-held light-polymerization unit (Elipar S10, 3M ESPE, St. Paul, USA) with a light intensity of 1200 mW/cm^2 for 40 s keeping the light curing tip in contact to the glass plate. The FRC ground samples were prepared by the same process, followed by grinding of the flat surfaces to approximately 0.2 mm with a 1200 grit (FEPA) silicon carbide grinding paper to expose the fibers. The substrates were then cleaned in deionized water in an ultrasonic cleaning device (Quantrex 90, L&R Ultrasonics) for 10 min and allowed to set under ambient laboratory conditions (23°C ± 1°C) for 60 min.

Next, the FRC intact and ground samples were divided into 2 groups based on the treatment agent of adhesive resin or primer used: a) StickRESIN adhesive and b) G-Multi PRIMER. Each group was further divided into 4 subgroups based on the application time of the adhesive resin or primer on the FRC substrate: 0.5, 1, 2, and 5 min protected from light. After the specified application times, the specimens were photo-polymerized again for 40 s in air, which led to the formation of an oxygen-inhibited layer on the surface (Bijelic-Donova et al., 2015).

4.4.2 Weight loss assessment

The weight of the specimens of each group (n=5, 4×3×1 mm^3) was measured to evaluate the weight loss caused by the evaporation of the liquid components of the adhesive resin or primer applied to the FRC substrate. The initial weight of the specimens was measured using a scale (ES 120A, Presica, Dietikon, Switzerland). Then, the adhesive resin or primer was applied to its surface while keeping the specimen on the scale to calculate the weight change of the adhesive resin and

primer. The specimen with the treatment solution was protected from light and kept on the scale for the specified adhesive resin or primer application times. The difference between the initial and final weights was calculated to determine the weight loss caused by the evaporation of the solvents of the monomers during the application time.

4.4.3 Surface microhardness test

Surface microhardness testing of the substrate surfaces (n=5, 4×3×1 mm^3) was performed on the surface with the resin luting material. A 0.3 mm thin layer of resin luting cement was applied over the FRC substrates and polymerized immediately. By using a Vickers hardness testing machine (Duramin-5; Struers, Westlake, OH, USA), a force of 980.7 mN was applied for 15 s to measure the surface hardness.

4.4.4 TBS test

TBS of the FRC-resin luting cement interface was measured using a universal testing machine (Model no. 3369 Instron, Canton, MA, USA) using specimens dried in air at room temperature. The test was performed at a cross-head speed of 0.5 mm/min using a 1 kN load cell. For fabrication of the TBS specimen, a mylar sheet was placed over a glass plate and over the mylar sheet the FRC sample was placed. Subsequently, the resin luting material (G-CEM LinkAce, GC, Tokyo, Japan) was spread on the mylar sheet on both sides of the FRC (in contact with the FRC), placing the FRC in the middle, like a sandwich, to have resin-FRC-resin. Before light-curing the sandwich, another mylar sheet was placed on top of the sandwich. Over the mylar sheet, a glass plate was also placed, followed by photo polymerization for 40 s. Once the samples were light-cured, the sample blocks were sectioned with a precision diamond saw (Isomet 5000; Buehler Ltd., Lake Bluff, IL, USA) at 1400 rpm under water cooling to a dimension of 12.0 mm x 1.0 mm x 1.0 mm (Figure 16). A bar-shaped specimen from each group (n=6) was glued to the grips of a tensile device with cyanoacrylate (Super Glue, Henkel/Loctite, Westlake, OH, USA), and the proprietary software was used to record the failure loads in newton (N) and the bond strengths in megapascal (MPa) (Figure 17).

Figure 16. Bar shaped samples for TBS testing.

Figure 17. TBS sample glued to the grips of a tensile device.

4.5 Statistical analyses

The available data from studies I-IV were statistically analyzed using SPSS ver. 23.0 for Windows (SPSS Corporation, Chicago, IL, USA). In all studies, an analysis of variance (ANOVA) test at the significance level of $p \leq 0.05$ was employed followed by Tukey's *post hoc* analysis for pair-wise comparisons. However, linear regression analysis (in Studies I, III & IV) and Pearson's correlation (in study III) were performed to validate the findings. Additionally, the Shapiro-Wilk test and Kolmogorov–Smirnov test ($p=0.05$) were used to confirm data for normality. Levene's test was also carried out for the equality of variance ($p=0.05$).

In study I, two-way ANOVA was employed to check the effect of two independent factors, *i.e.*, storage conditions and FRC surfaces on the dependent variable, *i.e.*, nanohardness of the matrix of FRC. Additionally, the regression model was explored to find the association between nanohardness and different FRC surfaces. Initially, all the data were checked for normality and homogeneity of variance using the Shapiro-Wilk, Kolmogorov-Smirnov and Levene's test ($p=0.05$).

Study II explored the effect of independent factors (adhesive/primer and aging duration) on dependent factors (nanohardness and elastic modulus of FRC) using a two-way ANOVA test. DC% of the resin luting material was also estimated with a two-way ANOVA test.

In study III, both descriptive (means and standard deviations) and inferential statistics (two-way ANOVA, linear regression analysis, Pearson correlation) were used. Two-way ANOVA was employed to estimate water sorption and TBS of FRC against independent factors (adhesive/primer and aging duration). While, linear regression and Pearson correlation tests were employed to perceive a relationship between TBS data and nanohardness data of study II.

In study IV, the three-way ANOVA test was used to evaluate TBS between FRC and resin luting material. The independent factors were (adhesive/primer, application time and FRC surface). The effect of adhesive/primer's application time on TBS was further studied using linear regression models.

Additionally, the adhesive interface of the samples was visually analyzed in study II for poorly polymerized PMMA phase and fracture patterns were evaluated in study III. Fracture patterns were not statistically inspected.

5 Results

5.1 Mechanical (nanohardness and elastic modulus) properties of FRC resin matrix (study I)

The nanohardness of the resin matrix of FRC was measured incrementally in "stages" (Table 3). Although, aging conditions of FRC had no significant effect on the nanohardness ($p=0.374$). However, evaluation of incremental nanohardness in stages was significantly diffferent ($p<0.001$). The interactive effect of aging conditions and stages of FRC from top to core was also found to be significant ($p=0.001$). The *post hoc* Tukey's test for pairwise comparisons found no significant difference within the fresh-group. However, statistical differences were observed within the ageing and FRC stages groups stored for 6-months and 2-years.

Table 3. Nanohardness values of resin matrix of FRC stored for various lengths of time before curing. Stages 1 to 5 refer to the depth of the measurement from the surface toward core of the material. Modified from original publication I.

Aging duration	Nanohardness (GPa)				
	Stage 1	**Stage 2**	**Stage 3**	**Stage 4**	**Stage 5**
2-weeks	$0.12 \pm 0.03_{a,b}$	$0.13 \pm 0.04_{d,e}$	0.13 ± 0.07	0.17 ± 0.09	0.17 ± 0.09
6-months	$0.08 \pm 0.05^{A,B}{}_{a,c}$	$0.08 \pm 0.05^{C,D}{}_{d}$	0.13 ± 0.10^{E}	$0.19 \pm 0.12^{A,C,F}$	$0.29 \pm 0.18^{B,D,E,F}$
2-years	$0.06 \pm 0.02^{G}{}_{b,c}$	$0.07 \pm 0.03^{H}{}_{e}$	0.13 ± 0.09^{I}	0.14 ± 0.11^{J}	$0.28 \pm 0.24^{G,H,I,J}$

Key: Same superscript uppercase letters demonstrate significant differences within the group ($p<0.05$). Same subscript lowercase letters demonstrate significant differences between the groups ($p<0.05$).

Elastic modulus for 2-weeks group was observed lower at stage 1, *i.e.*, matrix of the top surface of FRC than in the matrix of inner core. However, the difference between the elastic modulus at the surface compared to the inner core became more evident due to aging of the prepreg FRC. The aging conditions ($p<0.000$), incremental stages ($p<0.000$) and their interactive effect ($p<0.000$) had a significant effect on the elastic modulus of FRC. The details are presented in Table 4.

Table 4. Elastic modulus values of resin matrix of FRC stored for various lengths of time before curing. Stages 1 to 5 refer to the depth of the measurement from the surface toward the core of the material. Modified from original publication I.

Aging duration	Elastic modulus (GPa)				
	Stage 1	Stage 2	Stage 3	Stage 4	Stage 5
2-weeks	$2.49 \pm 0.18^{A,B,C,D}{}_{a}$	$2.99 \pm 0.24^{A,E,F}{}_{c,d}$	$2.81 \pm 0.19^{B,G,H}{}_{e}$	$3.50 \pm 0.29^{C,E,G}{}_{g,h}$	$3.58 \pm 0.32^{D,F,H}{}_{j,k}$
6-months	$2.19 \pm 0.23^{I,J,K}{}_{a,b}$	$2.22 \pm 0.28^{L,M,N}{}_{c}$	$2.93 \pm 0.41^{I,L,O,P}{}_{f}$	$4.26 \pm 0.79^{J,M,O,Q}{}_{g,i}$	$5.62 \pm 1.27^{K,N,P,Q}{}_{j,l}$
2-years	$2.51 \pm 0.54^{R,S,T}{}_{b}$	$2.26 \pm 0.63^{U,V,W}{}_{d}$	$5.73 \pm 1.09^{R,U,X}{}_{e,f}$	$6.14 \pm 1.81^{S,V,Y}{}_{h,i}$	$8.28 \pm 2.19^{T,W,X,Y}{}_{k,l}$

Key: See table 1

The contributing effect of the material's different stages to the total variability in the nanohardness was observed low (R^2=0.2) in the regression analysis test. However, the regression coefficient was detected as significant (0.039, $p<0.05$). Figure 18 illustrates association between the nanohardness of the resin matrix of FRC stored for various lengths of time before curing against different depth of the measurement (stages 1–5).

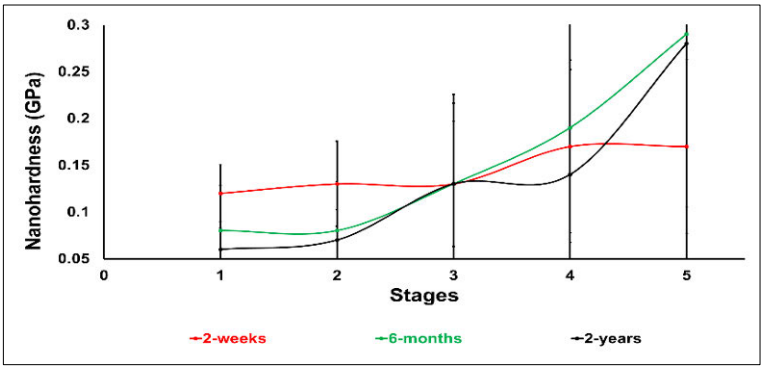

Figure 18. Relationship between dependent variable, *i.e.*, nanohardness of the resin matrix of FRC stored for various lengths of time before curing plotted against the depth of the measurement (stages 1–5), *i.e.*, from the surface toward the core of the FRC.

5.2 Chemical (Raman and XRD) properties of FRC resin matrix (Study I)

The Raman spectra suggested bond deformation of C-C-O and C-C-C at 500 cm^{-1}. Peaks observed in the range 730 to 850 cm^{-1} are associated with Si-O stretching (Khan et al., 2017c). Irrespective of the aging conditions, the core of the FRC demonstrated increased intensity (in the range 1600–1750 cm^{-1}) compared to top surface of the same group. Additionally, asymmetric and symmetric deformation in the plane of CH_2 was observed on the top surface of each group (1350 to 1450 cm^{-1}).

Both aromatic (C=C) and aliphatic (C=O) bond bands were observed in the range of 1650 to 1750 cm^{-1}, respectively (Figure 19). The XRD patterns of the resin matrix of stage 1 and stage 5 of FRC indicated that the polymer was amorphous without a long-range atomic order. Only a broad scattering peak (2q=40) was observed in each group. Figure 20 shows the XRD patterns of each group at stage 1 and 5.

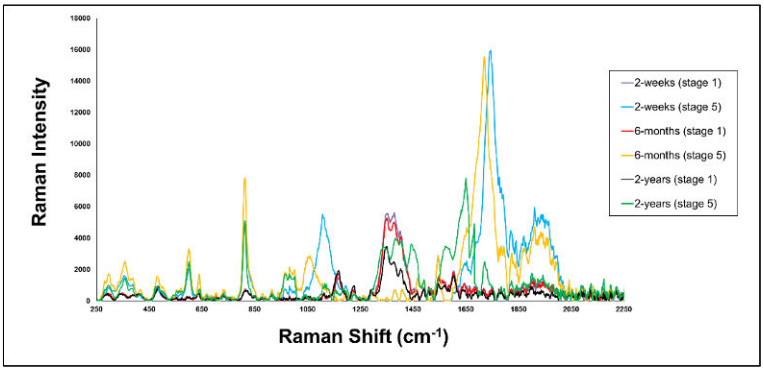

Figure 19. Raman spectra: “stage 1” and “stage 5” of the surfaces cured from FRC prepregs that were stored for various lengths of time before curing.

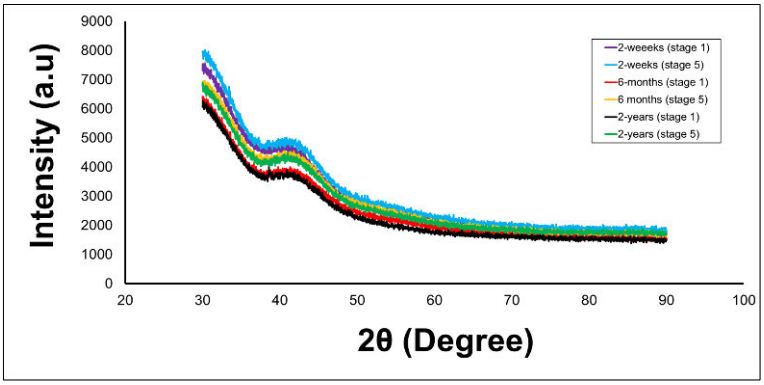

Figure 20. X-ray diffraction patterns: “stage 1” and “stage 5” of the surfaces cured from FRC prepregs that were stored for various lengths of time before curing.

5.3 Thermal (TGA and DSC) properties of FRC resin matrix (Study I)

Thermal stability data of stage 1 and stage 5 surfaces were observed to be similar. The TGA curves for both stage 1 and stage 5 surfaces started weight loss at 320°C, irrespective of the aging conditions. By the time the temperature reached to 420°C, the polymeric weight content from FRC was completely lost. However, no weight

changes were observed in glass-fiber content of FRC (Figure 21). Likewise, the DSC data also indicated insignificant effect of the temperature on FRC surfaces, irrespective of the aging groups. The Tg values of the all the groups were ≈ 200ºC (Figure 22).

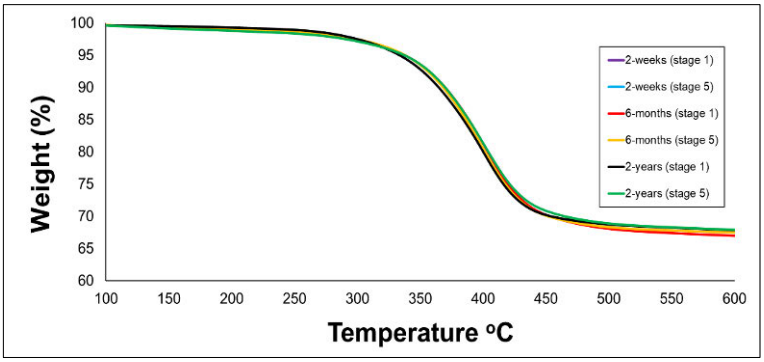

Figure 21. TGA curves: "stage 1" and "stage 5" of the surfaces cured from FRC prepregs which were stored for various lengths of time before curing.

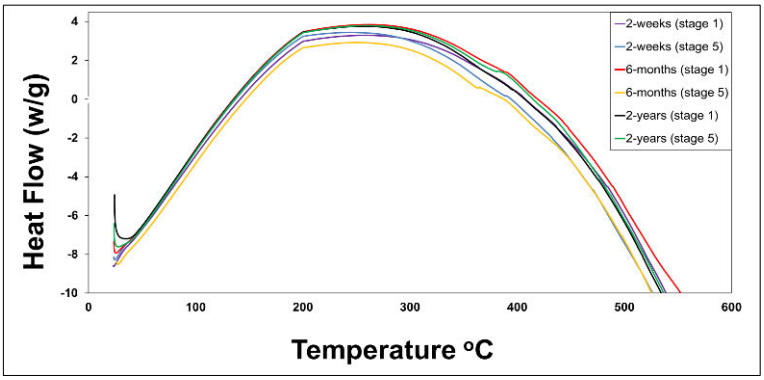

Figure 22. DSC thermograms depicting heat flow at: (A) surfaces of "stage 1" and "stage 5" of the FRC prepregs stored for various lengths of time before curing.

5.4 Degree of conversion (DC%) (Study II)

The DC% of resin luting material, *i.e.*, LinkAce was 41.3%. The effect of FRC used underneath resin luting material, with or without the adhesive/primer was also observed as insignificant. The details are presented in Figure 23.

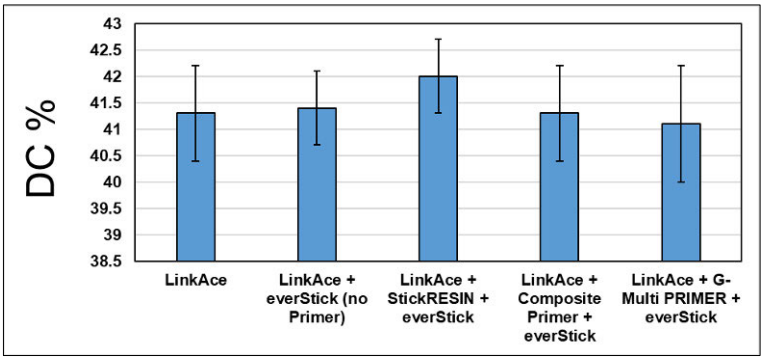

Figure 23. Degree of conversion (in %) of resin luting material in combination with adhesive/primer and FRC.

5.5 Mechanical properties of adhesive interface between resin luting material and FRC (Study II and III)

The two-way ANOVA data for both nanohardness and elastic modulus revealed that priming ($p<0.001$), aging conditions ($p<0.001$) and their interactive effect ($p<0.001$) had a significant effect on the nanohardness and elastic modulus of the adhesive interface of FRC. Additionally, the *post hoc* Tukey's test for pair-wise comparisons revealed statistical differences within and between the study groups ($p<0.05$). The highest nanohardness and elastic modulus were observed in 1.0-year and 1.5-year-aged G-Multi PRIMER primed FRC respectively, *i.e.*, 0.55 ± 0.21 GPa and 14.27 ± 5.19 GPa, respectively. The lowest nanohardness and elastic modulus were observed in 3.0-year-aged G-Multi PRIMER primed FRC, *i.e.*, 0.06 ± 0.05 GPa and 3.78 ± 2.74 GPa, respectively. Figures 24 & 25 present the graphical data of the study groups.

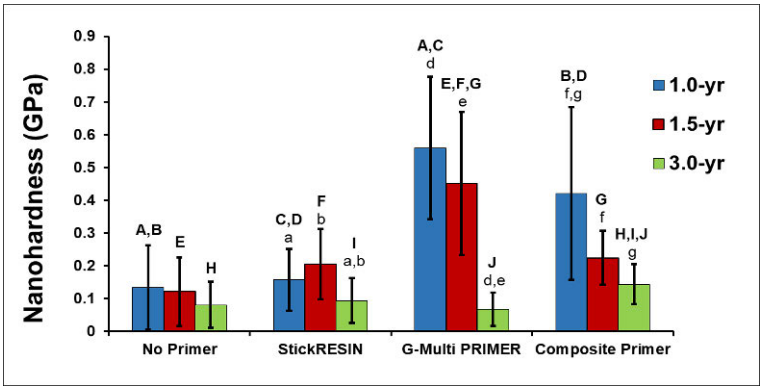

Figure 24. Nanohardness values of the adhesive interface between resin luting material and FRC using different adhesive/primers. Key: The same superscripted uppercase letters demonstrate significant differences between the material groups ($p<0.05$). The same subscripted lowercase letters demonstrate significant differences between the aging groups ($p<0.05$). Adopted from original publication II.

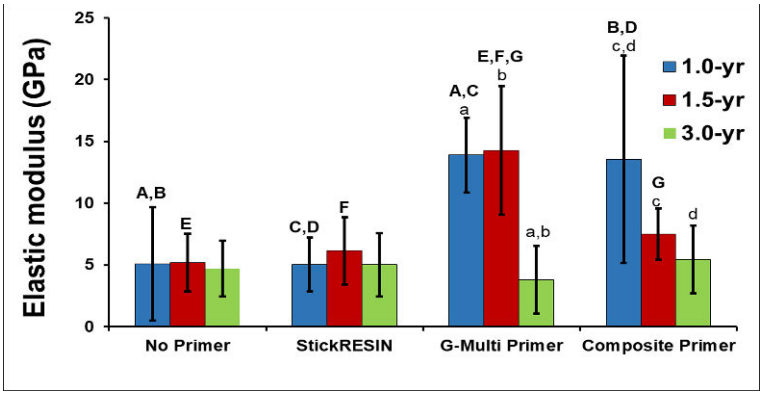

Figure 25. Elastic modulus values of the adhesive interface between resin luting material and FRC using different adhesive/primers. Key: See Figure 24. Adopted from original publication II.

The aging duration and the type of adhesive/primer used had significant effects on the TBS between the resin luting material and the FRC ($p<0.001$). The interactive effect of both aging duration and the adhesive/primer used was also witnessed as significant ($p<0.01$). The *post hoc* Tukey's test further affirmed significant differences between no primer and G-Multi PRIMER and between StickRESIN and G-Multi PRIMER in the groups aged for 1.0 and 1.5 years. At the end of 3.0 years of aging, G-Multi PRIMER was observed to have a statistically higher TBS (15.5 ± 2.7 MPa) compared with no primer (9.1 ± 1.2 MPa) or Composite Primer (10.2 ± 2.3 MPa). The details are given in Table 5.

Table 5. Tensile bond strength (TBS) for the groups investigated in Study III. Modified from original publication III.

Aging duration	Tensile bond strength (MPa)			
	No primer	StickRESIN	G-Multi PRIMER	Composite Primer
1.0-year	18.4 ± 1.6^{Aa,b}	21.1 ± 3.7^{Bd,e}	28.0 ± 2.9^{A,Bf,g}	23.1 ± 5.6^{h}
1.5-year	12.4 ± 1.3^{C,Da,c}	14.0 ± 2.0^{E,Fd}	17.5 ± 2.4^{C,Ef}	17.9 ± 2.8^{D,Fi}
3.0-year	9.1 ± 1.1^{G,Hb,c}	13.9 ± 1.0^{Ge}	15.5 ± 2.7^{H,Ig}	10.2 ± 2.3^{Ih,i}

Key: See Figure 24.

The regression analysis indicated a positive linear relationship between the nanohardness and TBS ($p<0.001$). A corrected R^2 value of 0.265 was observed with the statistical difference at $p\leq0.05$ (Table 6). Similarly, the Pearson correlation coefficient value was determined to be 0.51, signifying a strong correlation between the nanohardness and TBS (Table 7). The correlations between nanohardness and TBS are presented graphically in Figure 26.

Table 6. Linear regression coefficient table between nanohardness (Study II) and TBS (Study III). Adopted from original publication III.

Model	Unstandardized coefficients	Standardized coefficients	t	Sig.
	Std. Error	Beta		
(Constant)	0.93		14.27	0.000
(GPa)	3.13	0.514	5.02	0.000

Table 7. Pearson correlation matrix between nanohardness (Study II) and TBS (Study III). Adopted from original publication III.

		(GPa)	(MPa)
(GPa)	Pearson correlation Sig. (2-tailed) N		0.514** < 0.001 72
(MPa)	Pearson correlation Sig. (2-tailed) N	0.514** < 0.001 72	

*Correlation is significant at the 0.01 level (2-tailed).

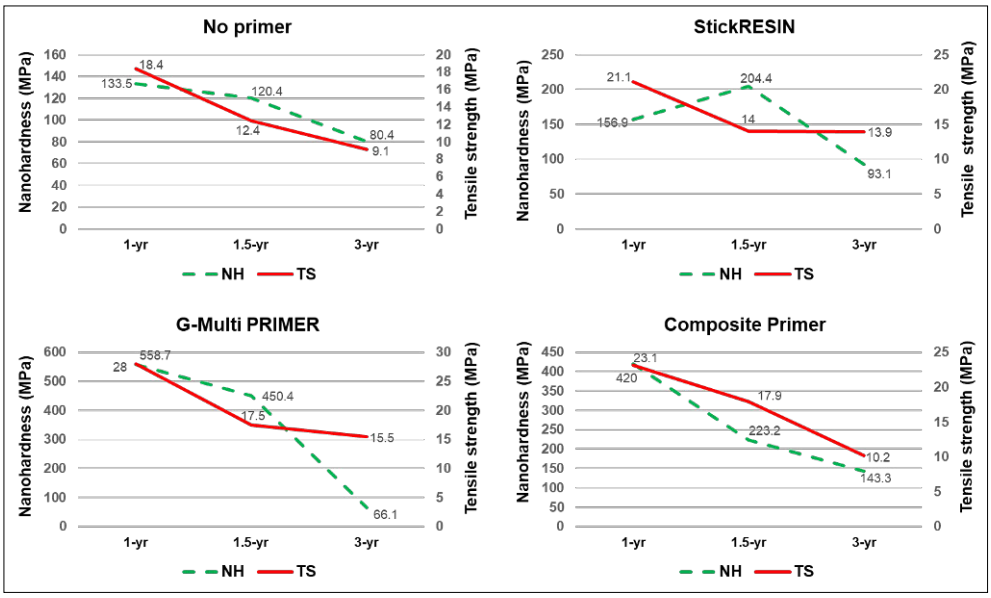

Figure 26. Correlation graphs between nanohardness (NH) and tensile bond strength (TS) using adhesive/primer and aging durations. Modified from original publication III.

5.6 Chemical properties of adhesive interface between resin luting material and FRC (Study II)

The ratio of formation of double bonds between C=C aromatic and C=C aliphatic compounds of FRC was determined as a function of adhesive/primer and aging of FRC. G-Multi PRIMER primed FRC exhibited the highest ratio when aged for 1.0-year (2.81). G-Multi PRIMER also exhibited the largest difference in the ratio between 1.0- and 3.0-year-aged groups. The lowest ratio was observed in 3.0-year-aged FRC no primer group (1.80). The smallest difference in the ratio was observed between 1.0- and 3.0-year-aged groups when StickRESIN was used. The details are given in Table 8.

Table 8. Change in the average intensity ratio between C=C aromatic and C=C aliphatic compounds of the tested groups. Modified from original publication II.

Aging condition	Average intensity ratio of C=C aromatic/C=C aliphatic compounds of FRC			
	No primer	StickRESIN	G-Multi PRIMER	Composite Primer
1.0-year	2.27	2.32	2.81	2.70
1.5-year	2.01	2.37	2.54	2.34
3.0-year	1.80	2.11	1.83	2.07

5.7 Visual evaluation of adhesive interface between resin luting material and FRC (Study II)

The adhesive interface of FRC was evaluated before and after being dissolved with THF. The visual analysis of the adhesive interface of 1.0-year-aged FRC with no primer before THF treatment showed smooth surface without any apparent margins between the resin luting material and FRC (Figure 27A). However, the 3.0-year-aged FRC with no primer exhibited gaps between the resin luting material and FRC after the THF treatment (Figure 27B). Similarly, gaps were also observed in the adhesive interface of 3.0-year-aged FRC with G-Multi-Primer (Figure 27C). All other groups demonstrated minor (if any) gaps after the THF treatment.

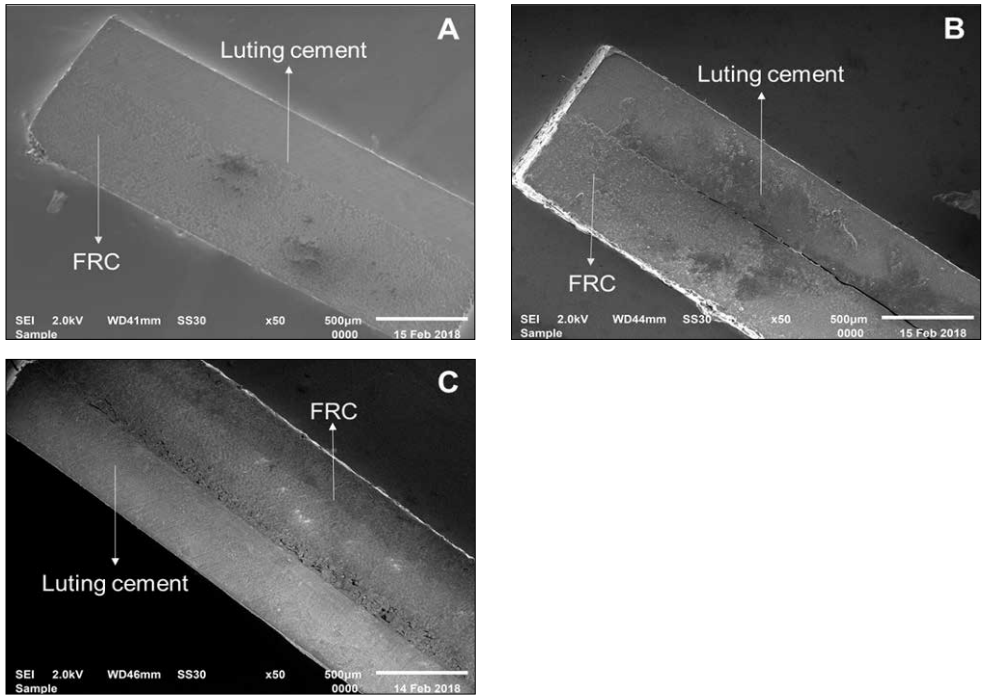

Figure 27. SEM images of the adhesive interface: A) 1.0-year-aged FRC with no primer before treating with THF; B) 3.0-year-aged FRC with no primer after THF treatment; C) 3.0-year-aged FRC with G-Multi PRIMER after THF treatment. Original magnification 50×, bar = 500 µm. Adopted from original publication II.

5.8 Water sorption (Study III)

The mean water sorption values are presented in Table 9. The water sorption values among the different groups varied from 19.2 ± 9.3 to 25.7 ± 4.3 µg/mm^3. According

to the ISO 4049 standards for water sorption of polymer-based materials, water-sorption values under the limit of 40 mg mm^{-3} values are considered acceptable (Müller et al., 2017).

Table 9. Mean water sorption values of the study groups (adopted from original publication III)

Aging duration	Water sorption (µg/mm^3)			
	No primer	StickRESIN	G-Multi PRIMER	Composite Primer
1.0-year	19.2 ± 9.3	23.0 ± 4.6	19.7 ± 9.9	23.1 ± 4.4
1.5-year	23.6 ± 7.2	21.1 ± 12.0	22.1 ± 11.2	17.5 ± 6.2
3.0-year	21.9 ± 8.3	25.7 ± 4.3	23.3 ± 10.1	22.7 ± 7.5

5.9 Fracture behavior of resin luting material and FRC joint (Study III)

Most failures were adhesive (Table 10). Adhesive failures were dominant for the FRCs with no primer, irrespective of the aging time. However, mixed and cohesive failures were witnessed when G-Multi PRIMER and Composite Primer were used. At the end of 3.0-year of aging, G-Multi PRIMER showed 16.7% mixed failure, while all the other groups demonstrated 100% adhesive failure. The images of the fracture modes are displayed in Figure 28.

Table 10. Failure mode distribution among the study groups (adopted from original publication III)

	Aging duration								
	1.0-year			1.5-year			3.0-year		
	AD	MI	CO	AD	MI	CO	AD	MI	CO
Groups	%			%			%		
No primer	83.3	16.7	0	100	0	0	100	0	0
StickRESIN	66.6	16.7	16.7	100	0	0	100	100	0
G-Multi PRIMER	50.0	33.3	16.7	66.6	16.7	16.7	66.6	16.7	16.7
Composite Primer	50.0	33.3	16.7	83.3	16.7	0	100	0	0

AD = adhesive failure, MI = mixed failure, CO = cohesive failure.

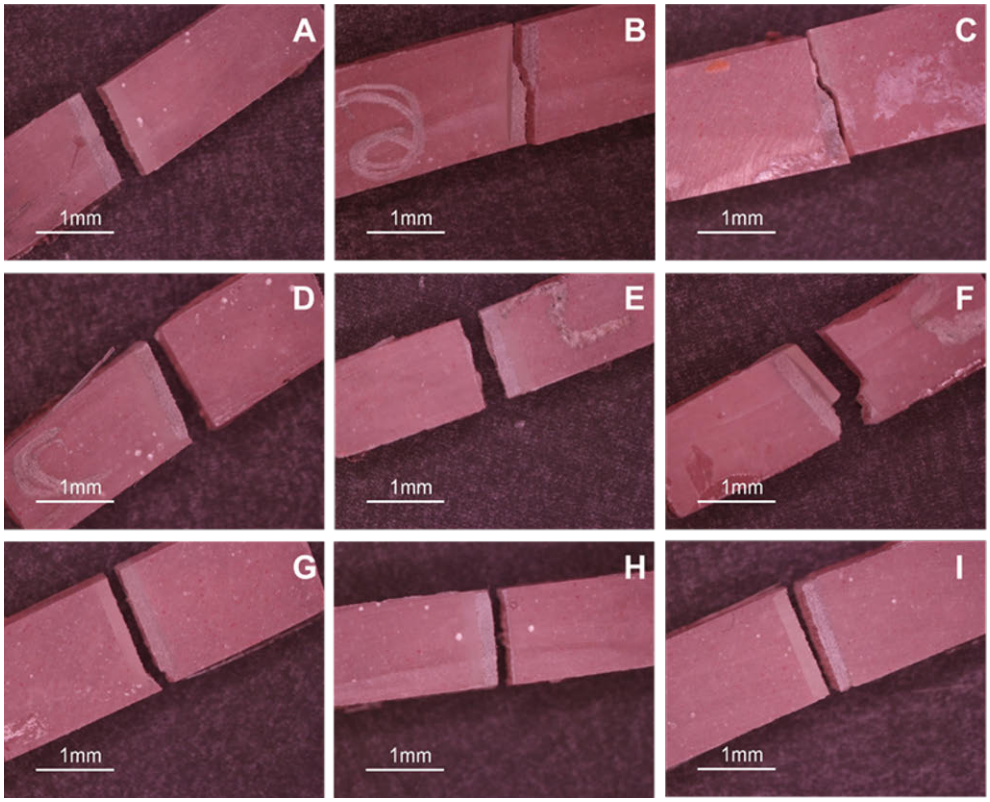

Figure 28. Stereomicroscopic images of samples using prepregs aged for 1.0-year (A–C). A: adhesive failure with no primer; B: mixed failure with G-Multi PRIMER; C: mixed failure with Composite Primer. Images of samples using prepregs aged for 1.5-year (D–F). D: adhesive failure with StickRESIN; E: cohesive failure with G-Multi PRIMER; F: mixed failure with Composite Primer. Images of samples using prepregs aged for 3.0-year (G–I). G: adhesive failure with StickRESIN; H: cohesive failure with G-Multi PRIMER; I: adhesive failure with Composite Primer. Adopted from original publication III.

5.10 Weight loss of monomers and solvents from adhesive/primer (Study IV)

The G-Multi PRIMER applied to the FRC ground surface for 5 min showed the highest weight loss (86.0%), while the StickRESIN adhesive showed little or no vulnerability to evaporation (Figure 29). Hence, most of the FRC substrates treated with StickRESIN for different time points exhibited no (0%) weight loss within the limits of precision of the method.

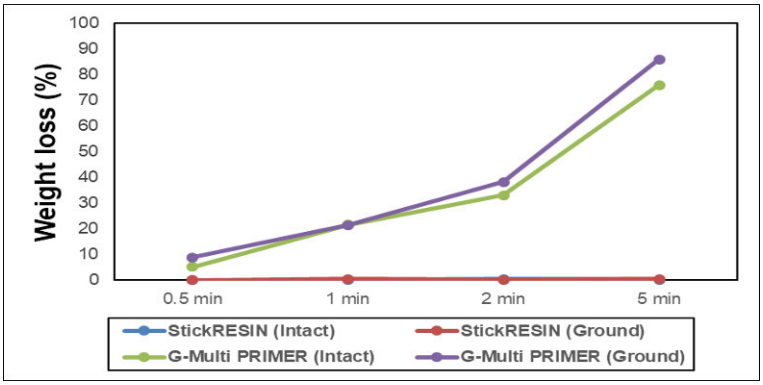

Figure 29. Weight loss of FRC (in %) as a function of evaporation of monomers and solvents at different time points. Adopted from original publication IV.

5.11 Vickers microhardness (VHN) of FRC ground and intact surfaces (Study IV)

A noticeable change in Vickers hardness was perceived for the resin luting material applied on top of the treated FRC intact or ground surfaces. The highest Vickers hardness was documented for the FRC ground surface treated with G-Multi PRIMER for 0.5 min, while the lowest was noted for the FRC intact surface treated with StickRESIN for 2 min. In general, the hardness increased with increasing treatment time of the FRC substrate by the adhesive/primer (Table 11, Figure 30).

Table 11. Hardness of resin luting material applied on top of the treated FRC intact or ground surfaces as a function of adhesive/primer application time. Adopted from original publication IV.

Treatment time	Vickers Hardness Number (VHN)			
	G-Multi PRIMER (Intact)	G-Multi PRIMER (Ground)	StickRESIN (Intact)	StickRESIN (Ground)
0.5 min	$21.3 \pm 1.1^{A,B}$	$24.6 \pm 1.4^{A,C,D}$	$14.7 \pm 0.5^{B,C,E}{}_{a}$	$20.1 \pm 1.2^{D,E}{}_{d}$
1.0 min	$20.7 \pm 0.8^{F,G,H}$	$24.0 \pm 0.4^{F,I,J}$	$14.4 \pm 0.3^{G,I,K}{}_{b}$	$19.6 \pm 0.8^{H,J,K}{}_{e}$
2.0 min	$20.2 \pm 1.4^{L,M}$	$23.9 \pm 0.3^{L,N,O}$	$14.3 \pm 0.3^{M,N,P}{}_{c}$	$20.7 \pm 0.6^{O,P}{}_{f}$
5.0 min	$20.6 \pm 1.7^{Q,R,S}$	$24.1 \pm 1.5^{Q,T}$	$18.1 \pm 0.5^{R,T,U}{}_{a,b,c}$	$23.1 \pm 0.5^{S,U}{}_{d,e,f}$

Key: Same superscript uppercase letters demonstrate the significant difference between the FRC surfaces and priming groups ($p \leq 0.05$). Same subscript lowercase letters demonstrate the significant difference between the different treatment time groups ($p \leq 0.05$).

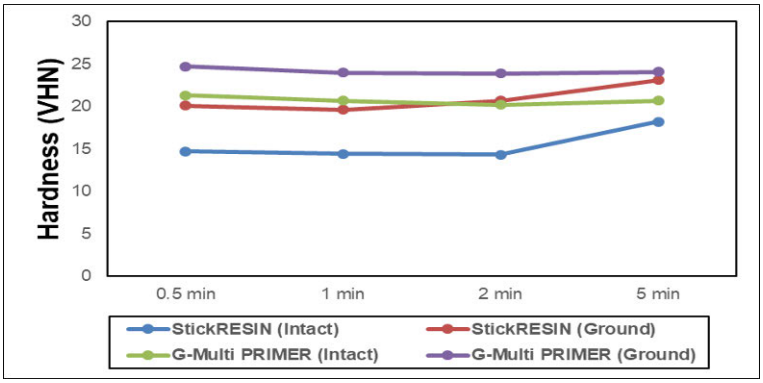

Figure 30. Hardness of resin luting material applied on top of the treated FRC intact or ground surfaces as a function of adhesive/primer application time. Adopted from original publication IV.

5.12 TBS of FRC intact or ground surfaces with resin luting material (Study IV)

Three-factor ANOVA revealed significant differences in TBS due to independent variables: FRC surfaces (intact or ground) ($p<0.001$), adhesive/primers ($p=0.047$), and treatment time ($P=0.010$). The interactive effect of the predictor variables such as FRC surface and adhesive/primer had a significant effect on TBS ($p<0.001$). However, the interactive effect of the FRC surface and the treatment time; adhesive/primer and the treatment time; and the joint effect of FRC surface, adhesive/primer and treatment time, had an insignificant effect on TBS ($p>0.05$). The details are in Table 12.

Table 12. TBS of the study groups wherein resin luting material applied on top of the treated FRC intact or ground surfaces as a function of adhesive/primer application time. Adopted from original publication IV.

	Tensile bond strength (MPa)			
Treatment time	**G-Multi PRIMER (Intact)**	**G-Multi PRIMER (Ground)**	**StickRESIN (Intact)**	**StickRESIN (Ground)**
0.5 min	$9.0 \pm 2.0^{A}{}_{a,b}$	$3.5 \pm 2.0^{A,B,C}{}_{d,e,f}$	9.5 ± 1.1^{B}	8.4 ± 2.0^{C}
1.0 min	$9.5 \pm 1.9^{D}{}_{c}$	$6.0 \pm 1.0^{D}{}_{d}$	9.3 ± 1.5	8.4 ± 2.8
2.0 min	$13.0 \pm 1.2^{E}{}_{a,c}$	$5.9 \pm 0.9^{E,F,G}{}_{e}$	10.1 ± 3.1^{F}	9.9 ± 2.6^{G}
5.0 min	$12.3 \pm 1.7_{b}$	$7.4 \pm 0.5_{f}$	10.9 ± 4.9	9.0 ± 4.8

Key: See Table 11

The regression analysis revealed that the correlation coefficients (R) of the G-Multi PRIMER for the FRC intact surface ($R=0.657$) and FRC ground surface ($R=0.731$)

were high. The treatment time affected both the G-Multi PRIMER-treated FRC intact and FRC ground surfaces, which led to an increase in TBS. However, StickRESIN on FRC intact or ground surface found to have no correlation (R=0.197 and R=0.118, respectively). The details are presented in Table 13.

Table 13. Linear regression model according to the treating conditions to ascertain the consequence of treatment time on FRC intact and FRC ground surfaces. Adopted from original publication IV.

Groups	Model	R	R Square	Adjusted R Square	Std. Error of the Estimate	Change Statistics			
						R Square Change	F Change	df1	df2
G-Multi PRIMER (intact)	1	.657[a]	.431	.400	1.84373	.431	13.659	1	18
G-Multi PRIMER (ground)	1	.731[a]	.534	.508	1.30039	.534	20.648	1	18
StickRESIN (intact)	1	.197[a]	.039	-.015	2.90579	.039	.727	1	18
StickRESIN (ground)	1	.118[a]	.014	-.041	3.10458	.014	.256	1	18

Predictors: Treatment time

The regression coefficient table further revealed that G-Multi PRIMER remarkably affected TBS of FRC intact and ground samples ($p=0.002$ and $p<0.001$, respectively). However, the treatment time had an insignificant effect on TBS of FRC intact and ground samples using StickRESIN ($p>0.05$). The details are shown in table 14.

Table 14. Regression coefficient table showing positive and negative correlation between each predictor variable against treatment time. Modified from original publication IV.

GROUPS		Unstandardized Coefficients		Standardized Coefficients	t	Sig.
		B	Std. Error	Beta		
G-Multi PRIMER (intact)	(Constant)	7.554	1.010		7.480	.000
	Treatment time	1.363	.369	.657	3.696	.002
G-Multi PRIMER (ground)	(Constant)	2.753	.712		3.865	.001
	Treatment time	1.182	.260	.731	4.544	.000
Stick RESIN (intact)	(Constant)	8.720	1.592		5.479	.000
	Treatment time	.495	.581	.197	.852	.405
Stick RESIN (ground)	(Constant)	8.161	1.700		4.799	.000
	Treatment time	.314	.621	.118	.506	.619

Predictor variable: TBS

6 Discussion

This thesis is based on laboratory experiments to determine the dissolving capability of different monomers and adhesive/primers into pre-polymerized semi-IPN-based FRC, and the effect of monomer systems and their treatment time on the nanomechanical, chemical and thermal properties of the matrix system of FRC. Additionally, polymerized FRC surfaces with high and low-gradient PMMA were evaluated for TBS with a resin luting material.

6.1 Mechanical properties of polymer matrix of the FRC (Study I & II)

Semi-IPN FRCs have a matrix system with a precise volume of cross-linked and linear polymer. Over the shelf life of the FRC prepreg, potential changes in the polymer structure in terms of cross-linking density of the matrix might have an impact on the adhesive properties of the FRC (Kallio et al., 2001; Lastumäki et al., 2002; Mannocci et al., 2005). Potential risk for evaporation of monomers, initiator and activator compounds from FRC necessitated performing this research. In an attempt to evaluate this, **Study I** was planned and devised. **Study I** focused on evaluating the shelf life of FRC prepregs that had been stored for up to two years before curing. Characterization of the matrix system was performed nanomechanically, chemically and by thermal means. Since gradient structure of FRC may change with time before curing. The change could be due to diffusion of cross-linking monomers and dissolved PMMA molecules. Therefore, the changes of the polymer structure and cross-linking density were indirectly investigated through nanomechanical means. The differences of the nanomechanical properties of the top and core FRC surfaces in terms of surface nanohardness and elastic modulus were evaluated. Although, hardness is a useful characterization method (Sattler, 2010), nanoindentation is a more reliable and accurate computation technique to measure the unit area of the indented surface (Sattler, 2010).

The nanoindentation data of **Study I** went against the initial hypothesis and confirmed that the nanohardness and elastic modulus of the resin matrix of the top surface were lower in values than that of the resin matrix of the core surface of FRC stored for 6-months and 2-yr before curing. This suggests that higher PMMA

gradient is present in the core surface during the fabrication process of FRC prepregs. The nanohardness of the two-weeks group showed no statistical differences between the top and core surfaces. However, FRC prepregs that had been stored for 6-months and 2-years before curing showed statistically higher nanohardness and elastic modulus of the core surfaces compared to their corresponding top surfaces. This indicated that a higher cross-linking density of resin matrix is present in FRC prepregs of core surfaces aged for longer duration. Also, the data suggested that PMMA molecules concentrated by diffusing to the core of the FRC prepreg when FRC prepregs were aged for longer duration. Semi-IPN of everStick C&B is a heterogeneous phase-separated material where linear and cross-linked polymers are dual phase at molecular level (Sperling, 1981). When thermodynamic interaction between polymer components, kinetic motion, and mobility of polymer chains take place during diffusion, phase-segregation between the network chains may expedite, as found in **Study I** (Sperling, 1981). This unpredictable behavior might be due to comparatively inadequate stability of resin matrix components of this particular semi-IPN-based FRC, resulting in disintegration of dual-phases with aging of the FRC prepreg.

Some resin luting materials and uniquely composed primers with and without a photo-initiator system have been recently introduced to enhance adhesion of resin luting material with semi-IPN FRC. Although primers may have good dissolving capability of PMMA in the semi-IPN system, however, primers also contain solvents, which could have an adverse effect on the bonding properties of resin luting material and FRC. Therefore, **Study II** was envisaged to indirectly assess through nanoindentation the dissolving capability and solidification of the dissolved surface layer of the resin matrix of FRC by photo-activated cross-linking of the resin luting material on top of the FRC.

The working hypotheses were accepted as both the aging and the monomer systems of the adhesive/primers demonstrated a notable effect on the properties of the FRC. The nanohardness and elastic modulus data reflected the presence of linear PMMA at the interface rather than a cross-linked *bis*GMA in FRC prepregs stored for up to 3.0-year before curing. This could be explained by the diffusion gradient of cross-linking monomers and PMMA polymer chains during the shelf life of the prepregs. The findings of **Study II** are consistent with those of **Study I**. The surface adhesive properties of FRC prepregs stored for three years may have deteriorated with time (Khan et al., 2018a). For clinical survival, durable bonding between the prosthesis substructure and resin luting material is vital (Khan et al., 2017a; Khan et al., 2018c). Higher surface ratio of PMMA on the FRC prepreg could alter the surface properties of FRC when adhesive/primers of different kinds are used.

The lower nanohardness and elastic modulus values among samples of 3.0-year-aged groups might be explained by the higher gradient of PMMA on the FRC

surface, and thus at the adhesive interface. Another possible aspect could be the phase-segregation of the resin matrix of FRC. The presence of PMMA molecules in semi-IPN polymer network might reduce the cross-linking density of the resin system with time, and hence, the surface become prone to dissolution by adhesive/primers. Interestingly, curing the monomer components of the resin luting material or adhesive/primers could not enhance the nanohardness of the interface. Despite the fact that the solubility parameters of *bis*GMA (the main component of StickRESIN) and PMMA are close to each other (Mannocci et al, 2005), the dissolution might occur due to the presence of the photo-initiator system in StickRESIN; otherwise, *bis*GMA monomer would have been cured at the adhesive interface. The presence of PMMA or poorly polymerized resins at the interface was also confirmed via the dissolution test with the solvent THF. However, for the samples prepared with prepregs aged for shorter time, the surface nanohardness increased with the introduction of adhesive/primers to the interface.

In **Study II**, both G-Multi PRIMER and Composite Primer considerably increased the surface nanohardness and elastic modulus of 1- and 1.5-year-aged prepregs. Notably, these primers might not adequately photocure by themselves although they contained photo-initiators. The DC% estimation of the resin luting material using FTIR further affirmed that the primers or adhesive resin did not influence the polymerization process of the resin luting material when measured from a distance of ca 400μm. However, the DC% cannot be used to anticipate the hardness when different polymers are compared. The two systems may have similar hardness but remarkably different DC% (Dewald and Ferracane, 1987). Thus, the pivotal role of the adhesive/primers in **Study II** was to dissolve the surface of FRC and enhance the diffusion of monomers of resin luting material into the surface layer of FRC, which enabled the cross-linking of monomers and unsaturated methacrylate groups of *bis*GMA in the FRC with the monomers of resin luting material. Perea et al. found a similar dissolution capability using a Composite Primer (Perea et al., 2015). However, statistically non-different nanohardness and elastic modulus was observed between the control (no primer) and StickRESIN groups when their respective aged prepreg groups were compared, indicating that the monomers of the resin luting material or StickRESIN did not dissolve the FRC surface fairly. Moreover, if slight dissolution had occurred, the double bonds on the main polymer structure might have presented a large steric hindrance and low molecular mobility owing to its large molecular size, and the crosslinking may have been limited through free radical polymerization (Li et al., 2014). Therefore, it was deduced that the primary action of adhesive/primers was to dissolve the FRC surface. The primers enabled the monomers of the resin luting material to infiltrate the FRC surface and polymerize to form solid adhesive interface bonding between the FRC and resin luting material.

6.2 Chemical & thermal properties of FRC resin matrix (Study I)

In **Study I**, an initial attempt was made to chemically characterize the resin matrix of the FRC. FRC core surface revealed an increased intensity peak in the range from 1600 to 1750 cm^{-1} related to aromatic rings, suggesting a *bis*GMA rich core surface. In contrast, the top surface of FRC revealed very weak interaction, confirming the existence of a PMMA rich layer. However, marginal differences in the spectra of two-weeks and 2-year groups of FRC core need to be studied further to thoroughly understand the differences observed.

However, XRD analysis showed broad diffraction peaks linked with amorphous glass in all aged groups, irrespective of the top and core surfaces. The findings differ from the results with particulate filler resin luting material, where crystallinity of the resin luting material was found (D'alpino et al., 2014). In contrast, the major component of the semi-IPN polymer is amorphous *bis*GMA and TEGDMA, which inhibit the movement of polymer chains to crystallize. Therefore, if the crystallinity or semi-crystallinity would have been noticed, that would perhaps be due to the thermoplastic PMMA phase of the semi-IPN polymer. Although, isotactic PMMA has a tendency to crystallize (Ute et al., 1995). However, the amorphous polymer structure of PMMA used in this particular semi-IPN system was principally syndiotactic with a lower proclivity for crystallization (Ruyter and Svendsen, 1980). TGA findings revealed no variation in degradation between core and top surface. The degradation began around 290°C, and above 440°C the sample mass tended to stabilize, corresponding to glass fiber inorganic content. DSC test further revealed unremarkable thermal events e.g. crystallization, change in melting or glass transition temperature between core and surface of all tested groups. These results reflect the behavior of predominant thermoset components of the semi-IPN.

6.3 Chemical properties of the adhesive interface (Study II)

The average intensity ratios of the aromatic and aliphatic compounds were in agreement with the findings of nanoindentation data of **Study II**. The share of aromatic C=C bond is lowered as a function of aging of everStick, reflecting the reduced concentration of compound(s) containing an aromatic ring at the adhesive interface. Conversely, this can be viewed as the formation or existence of a PMMA layer at the adhesive interface. In the case of StickRESIN, the differences between 1.0- and 3.0-year-aged groups were not evident owing to the presence of *bis*GMA as a component of StickRESIN. However, a slight decrease in the intensity ratio as a function of aging of everStick was observed in the StickRESIN group, indicating the existence of a PMMA-rich layer.

6.4 TBS of adhesive interface between resin luting material and FRC (Study III)

An understanding of the influence of adhesive/primers infiltration into the FRC was obtained from **Study II**. However, Study **III** appraised the influence of the same adhesives/primers used in **Study II** on TBS between FRC and resin luting material, also the effect of these adhesive/primers on FRC prepregs aged for the same durations as used in **Study II** before curing.

The hypothesis of **Study III** was rejected because the monomer systems of the adhesive/primers used showed a notable effect on TBS between the resin luting material and the FRC substrate. The bond strength is a useful method to clinically predict the success of adhesion of dental restorations to tooth substances (Hamza et al., 2004; Ilday and Seven, 2011), therefore this testing method was selected to assess the bonding properties of resin luting material to FRC at different aging times during the shelf life of the FRC. TBS data indicated that the application of G-Multi PRIMER on the FRC substrate increased the bond strength of resin luting material to FRC. The presence of a reasonably substantial amount of ethyl alcohol in G-Multi PRIMER, which might swell the linear polymer in the semi-IPN system of the FRC; as a result, the phosphate ester monomer and dimethacrylate component of resin luting material penetrate into the semi-IPN structure for increased bonding. The presence of ethyl alcohol is notable for increasing the polymer chain mobility and radical diffusion rate (Cadenaro et al., 2010). The previous studies have thoroughly investigated the effect of ethyl alcohol on PMMA (Basavarajappa et al., 2016; Basavarajappa et al., 2017).

The higher TBS in Composite Primer group might advocate that the monomers in Composite Primer (2-hydroxyethyl methacrylate [HEMA, 30% to 60%; UDMA, 10% to 30%]) swelled the FRC surface and helped the penetration of resin luting material (G-Cem LinkAce). A logical basis could be the lower molecular weight (MW) and viscosity coefficient (η) of the monomers in Composite Primer: MW = 130.14 g/mol, d = 0.0057 Pa for HEMA; MW = 470 g/mol, d = 23 Pa for UDMA (Gajewski et al., 2012). However, upon aging of the prepreg, the crosslinking monomers might gradually lower in gradient of its surface and become enriched with PMMA molecules. Consequently, lower TBS was observed in aged groups.

While using a StickRESIN adhesive, the monomers of the resin luting material could not adequately infiltrate the FRC surface. *bis*GMA is a base monomer in StickRESIN with a molecular weight of 512 g/mol, which is considerably higher than that of HEMA and UDMA. Despite the high intrinsic reactivity of *bis*GMA, hydroxyl groups on the backbone and the interactions enabled by the aromatic rings increase the initial viscosity to d = 1200 Pa. The viscous primer resin may reduce monomer mobility during polymerization (Cadenaro et al., 2010; Cadenaro et al.,

2008), therefore, the end goal of dissolving the FRC surface could not be attained. Besides, the solubility parameters of *bis*GMA are close to those of PMMA. It is possible that the photoinitiator system in StickRESIN may have hindered the dissolution ability of *bis*GMA and thus lowered the TBS of the adhesive interface for this group (Khan et al., 2018b; Mannocci et al., 2005). **Study II** showed a marginally higher DC% at the interface between FRC and resin luting material when the resin luting material was used with StickRESIN adhesive and compared with the use of other primers (Khan et al., 2018b). However, it seems that there is no correlation between DC% and the TBS. Furthermore, the presence of 25% to 50% UDMA in G-Cem LinkAce luting material indicates that UDMA alone could not adequately swell the surface of the FRC substrate owing to its high molecular weight.

The TBS decreased with increasing aging time of the FRC prepregs in all the groups. The resin matrix in the prepregs might progressively change with time, resulting in the enrichment of the linear polymer at the interface. This change could be due to the diffusion of the crosslinking monomers and the dissolved PMMA molecules in the FRC prepreg. Consequently, overall TBS of resin luting material and FRC was lower for the prepregs aged for 3.0-year among all the adhesive/primer groups.

The thickness of the resin luting material might have affected the TBS of the material system. When the monomers of the resin luting material penetrate into the semi-IPN system of the FRC substrate, the interdiffusion zone has a lower crosslinking density than that of the cured resin luting material of the dimethacrylate system. Thus, the cured resin luting layer has a higher TBS compared to the interdiffusion zone between the FRC and the resin luting material. Additionally, the stress distribution between the resin luting material's thickness and different physical properties are also believed to affect the measured TBS. Besides, a slight variation in sample geometries might also effect the TBS. However, a recent study advocated that, for a given cross-sectional area and for any gauge length, disparity in the sample's shape and size have no effect on TBS (Masete et al., 2018).

Interestingly, a clear correlation between the TBS of **Study III** and the nanohardness of **Study II** was observed. A similar downward trend in the nanohardness values was also observed with the aging of the prepregs before their curing in **Study II** (Khan et al., 2018b). The lower R^2 value might be due to the use of StickRESIN, which showed increasing nanohardness at 1.5 years, whereas the TBS was lower at 1.0-year than at 1.5-year.

6.5 Failure mode (Study III)

The failure mode was observed to shift from adhesive to cohesive with a surge in interfacial bond strength between the resin luting material and the FRC. Both G-

Multi PRIMER and Composite Primer showed more mixed failures (33.3% and 16.7% after aging for 1 and 1.5 years, respectively) compared with the other groups. StickRESIN, G-Multi PRIMER, and Composite Primer all exhibited 16.7% cohesive failures with the prepreg aged for 1.0-year, indicating that the adhesion between the resin luting material and the FRC was stronger than the cohesive strength of the FRC substrate. However, cohesive failure for the prepregs with G-Multi PRIMER aged for 1.5 and 3.0-year suggests that the FRC components of the semi-IPN system might disintegrate during prolonged storage, resulting in the phase-segregation or decreased cohesive strength of the matrices.

6.6 Weight loss & surface microhardness (Study IV)

Study IV was designed in order to gain a better understanding of the PMMA gradients of the intact and ground surfaces. It is pivotal to eliminate the solvents before polymerization as residual solvents may impede and interfere with the curing process at the interfacial region (Nihi et al., 2009). Generally, acetone, ethanol, and water are used as solvents in commercially available adhesive/primers (Ikeda et al., 2005). G-Multi PRIMER was observed to vaporize at room temperature, perhaps due to the high concentration of ethyl alcohol used in G-Multi PRIMER's composition (up to 90%). Although the G-Multi PRIMER showed minimal evaporation at 0.5 min (5.08%) however, 85.95% weight loss was noticed at 5 min due to solvent evaporation. The evaporation of ethanol at 20°C is 5.95 kPa owning to the vapor pressure of ethanol. However, this pressure increases to 53.3 kPa at 63.5°C (Nasirzadeh et al., 2004). Since samples were tested at ≈ 23°C ± 1°C, at a higher room temperature, the evaporation might have been swift due to an increase in the vapor pressure of ethanol. On the other hand, the StickRESIN adhesive tended to penetrate the FRC substrate. This is probably due to the formulation of StickRESIN, which contains *bis*GMA, TEGDMA and an initiator system. This adhesive has a considerably low vapor pressure and does not contain any solvent.

Some basic mechanical features of a material can be determined using a relatively simple and effective surface microhardness technique (ChenLee and Ho, 1998; Kallio et al., 2014). The hardness data demonstrated that the FRC ground surfaces are harder than the FRC intact surfaces, irrespective of the treatment agent used. This can be ascribed to the peculiar feature of linear polymers, *i.e.*, ductility. PMMA is a ductile low hardness resin polymer, and its polymer chains are compelled together mainly by weak chemical bonds such as van der Waals forces. On the other hand, the copolymer of *bis*GMA-TEGDMA are held together by covalent bonds in the semi-IPN system. Since the PMMA gradient is higher in FRC

intact than in FRC ground (Basavarajappa et al., 2019), the hardness values of the FRC intact groups were lower than those of the FRC ground groups.

6.7 Interfacial TBS between resin luting material and polymerized intact and ground FRC surfaces (Study IV)

The working hypothesis of **Study IV** was rejected since the adhesive resin and primer manifested a significant effect on Interfacial TBS between resin luting material and polymerized intact and ground FRC surfaces. The use of G-Multi PRIMER on the FRC intact substrate enhanced TBS of the FRC to the resin luting material. The reason is the presence of an enriched PMMA layer. G-Multi PRIMER is mainly composed of ethanol that swells the PMMA, since the solubility parameter of ethanol (12.92 $(cal/cm^3)^{1/2}$) is near or similar to that of PMMA (8.9–12.7 $(cal/cm^3)^{1/2}$) (Basavarajappa et al, 2019). This may promote the diffusion of the phosphate ester monomers of the primer and the dimethacrylate component of the resin luting cement into the PMMA layer of the FRC. The polymer chain mobility and radical diffusion rate have already been determined using ethanol (Cadenaro et al., 2010), and the reaction of ethanol on PMMA has been examined in depth (Basavarajappa et al., 2016; Basavarajappa et al., 2017). Whereas, the bonding of the resin luting material to FRC ground was inadequate with the G-Multi PRIMER treatment. Perhaps this is because the intact FRC surface is comprised of 100% resin material, in contrast, the ground FRC surface consisted of 50% resin and 50% exposed silicate glass, *i.e.*, fiber. This indicates that the deficiency of the PMMA component in the FRC ground results in inadequate interaction with the phosphate ester monomer and the dimethacrylate component of the resin luting material.

The StickRESIN adhesive resin could not sufficiently diffuse into the PMMA-enriched FRC intact surface. As reported in the material data sheet, StickRESIN comprised of *bis*GMA, which has a molecular weight of 512 g/mol (Khan et al., 2019). The higher molecular weight might result in increasing the viscosity of the adhesive resin and lowering the mobility of *bis*GMA during curing (Cadenaro et al., 2010; Cadenaro et al., 2008). Besides, the photoinitiator system and the followed spontaneous polymerization initiation of StickRESIN might have prevented the dissolution by *bis*GMA (Khan et al., 2018b; Mannocci et al., 2005), as a result, the lower TBS of the adhesive interface for this group was observed, irrespective of the time for which the adhesive was applied to the FRC intact substrate. This is in line with previously published results (Kallio et al., 2003).

However, the TBS was found to be higher when the FRC ground surface was treated with StickRESIN and bonded to the resin luting material compared to that of the FRC ground surface treated with G-Multi PRIMER. The presence of a highly

cross-linked resin component in FRC ground is not instrumental in the formation of a strong bond between the resin luting material and FRC ground substrate. The dimethacrylate component of the resin matrix of FRC polymerizes to a highly cross-linked component (Kawaguchi et al., 2011b), and their high crosslinking density results in inadequate bonding of the resin luting material to FRC. In the semi-IPN structure with PMMA, the presence of PMMA enables the dissolution of the PMMA surface (Kawaguchi et al., 2011a). It is worth noting that the TBS test was employed in **Study IV**, not the so-called shear bond strength test, and thus, the findings in MPa cannot be compared to the reported bond strength tests. TBS testing has been proclaimed as more appropriate for studying the interfaces of dental materials (Della Bona and Van Noort, 1995; Rasmussen, 1996).

The linear regression model in the split mode clearly supports the effect of application time of G-Multi PRIMER on both FRC intact (R=0.657) and FRC ground (R=0.731) samples, presenting a linear association between treatment time and TBS. The non-linear association between treatment time and TBS using StickRESIN adhesive can imitate the inefficiency of dissolution by this type of adhesive resin on FRC surfaces.

6.8 Implications, clinical considerations and future perspectives

FRCs are mainly composed of polymeric materials, and their laboratory or clinical performance is related to the chemical structural arrangement, rate of degradation and shelf-life (Drummond, 2008). In this thesis, multiple important facts have been uncovered which are crucial for the current understanding and clinical practice. Firstly, the likely change and phase-segregation in the polymer structure related to cross-linking density of the resin matrix during aging were perceived and it was observed that the PMMA molecules concentrate by diffusion even more to the core of the FRC prepreg when the storage time prolongs. This gradient structure has a profound influence on the dissolving characteristics and the adhesion properties of the FRC. Secondly, the clinical performance of a FRC restoration is dependent on the dissolving capabilities of monomers and solvents present in the adhesive or primers to improve the penetration of monomers of resin luting material into the PMMA enriched surface layer of FRC for enhanced bonding. A secure and durable interface between the resin luting material and FRC is essential to transfer the stress and load from the resin luting material to the FRC-based prostheses, and also guarantees the clinical success of FRC-based prostheses. Thirdly, the elimination of solvents before light curing is crucial since residual solvents may deteriorate and interfere with the polymerization process at the adhesive interface of FRC.

Long-term clinical studies are needed to confirm the findings of this thesis. Since samples were tested immediately after polymerization, future studies should evaluate FRC substrates after subjecting them to thermocycling and artificial saliva storage for longer duration. While this thesis only included commercially available adhesive resin and primers composed of multiple monomers and other solvents, future studies of individual monomers are essential to rationalize the findings. In addition, only one type of resin luting material was used throughout the studies, the present findings need to be corrobated with other resin luting materials. Moreover, prospective clinical studies are required to evaluate whether the improved bonding in G-Multi PRIMER observed in **Study IV** corresponds to enhanced clinical performance.

7 Conclusions

Based on the studies included in this thesis, the following conclusions might be drawn:

1. The semi-IPN structure of everStick C&B is affected by the long-term storage of FRC prepreg before curing. The PMMA molecule concentration becomes higher in the core of FRC prepreg upon aging. The resin matrix of the semi-IPN FRC experiences a reduction in nanohardness and modulus of elasticity on the surface compared to in the core due to the long-term storage of FRC prepreg before curing.
2. The treatment of adhesive or primers on semi-IPN based FRC surface has no influence on the DC% of the resin luting material. FRC prepregs dry-aged for 3.0-year before curing exhibited the lower interfacial surface nanohardness, which may be explained by the higher ratio of PMMA at the interface. For 1.0- and 1.5-year-aged prepregs and for the corresponding FRC, the most durable adhesive layer was obtained when the G-Multi PRIMER or Composite Primer were used. Both G-Multi PRIMER or Composite Primer might have the ability to form a solid adhesive interface bonding between the FRC and the resin luting material.
3. It is likely that the shelf-life of the semi-IPN based FRC prepreg and the priming systems both influence TBS between resin luting material and FRC substrate. Both G-Multi PRIMER and Composite Primer showed enhanced TBS with prepregs aged for 1.0- and 1.5-year. Only G-Multi PRIMER showed higher TBS with prepregs aged for 3.0-year. The lower TBS with older prepregs for all primer conditions might suggest a diffusion-related change of the semi-IPN resin matrix before the prepreg was used.
4. Prolonging the application time of adhesive resin or primer on semi-IPN based FRC surfaces may enhance the TBS between the resin luting material and FRC, irrespective of the treatment agent used. The highest TBS between the FRC and resin luting material can be obtained with the G-Multi PRIMER treatment with 5 min evaporation time of the solvent of the primer.

Acknowledgements

Undertaking a risky and daring journey of completing PhD was not less than a life-changing experience for me, and it would not have been attainable without guided directions and suggestions that I received from many people during my years of PhD, *i.e.,* 2017-2020.

Firstly, I would like to signify the importance of Prof. Pekka Vallittu in my life, whose constant and endless support, patience, motivation, and immense knowledge paved the way to start my training as a researcher. Conducting the research studies on such a challenging research area couldn't be as simple as he made this for me. With exaltation, his wisdom, knowledge, expertise, motivation, and encouragement helped me during the research and writing of this thesis. Indeed, one cannot imagine having a better advisor and mentor for one's Ph.D. study than him. Unquestionably, without Prof. Pekka Vallittu's invaluable guidance and support this thesis would not have existed. Undoubtedly, Prof. Vallittu, I am extremely enlightened by your wisdom, knowledge, understanding and expertise.

Besides my Ph.D. supervisor, I am equally thankful to Eija Säilynoja (my co-supervisor), whose knowledge and understanding of chemistry is outstanding. Eija, without your help and support, interpretation of some results were simply impossible. Your insightful comments and hard questions incentivized me to widen my research from various perspectives.

My sincere thanks also goes to Prof. Abdulaziz AlKhureif, who recommeded my name and created a bridge between Prof. Pekka and I, and who allowed me to access all the laboratory and research facilities in the Dental Health Department, College of Applied Medical Sciences, King Saud University, Riyadh, Kingdom of Saudi Arabia, during 2017-2021. Prof. Abdulaziz, without your precious support, it would not have been possible to conduct these series of researches. I am greatly indebted to you.

I also want to express the gratitude to Dr. Leila Perea-Lowery for helping in fabrication of different dimensions' samples. I was very fortunate to have Prof. Badreldin Mohamed for statistical help and interpretation of difficult findings.

I would never forget my fellow lab mates for working together, helping each other, and sleepless nights that gave us the courage to complete goals and targets

within the time-frame. My warm thanks go to co-authors for their technical support, constructive comments, and proofreading of manuscripts.

In the end, I am grateful to my mother, sisters, friends and acquaintances who remembered me in their prayers for this ultimate accomplishment. I owe great gratitude to my beloved wife, Sanam for her care, love, encouragement and support during hard times. During this difficult period, you took care of our children, *i.e.*, Mustafa and Fatima without complaining a single time. This thesis would not have been possible without your warm love, continued patience, and endless support. Truly, you all are my sunshine of life.

19-2-2021
Aftab A. Khan

References

Abdulmajeed, A.A., Närhi, T.O., Vallittu, P.K., Lassila, L.V., 2011. The effect of high fiber fraction on some mechanical properties of unidirectional glass fiber-reinforced composite. *Dental Materials*, 27(4), p. 313–321.

Akovali, G. 2001. Handbook of Composite Fabrication, Smithers Rapra Publishing.

Alander, P., Lassila, L.V., Tezvergil, A., Vallittu, P.K., 2004. Acoustic emission analysis of fiber-reinforced composite in flexural testing. *Dental Materials*, 20(4), p. 305–312.

Altieri, J.V., Burstone, C.J., Goldberg, A.J., Patel, A.P., 1994. Longitudinal clinical evaluation of fiber-reinforced composite fixed partial dentures: a pilot study. *The Journal of Prosthetic Dentistry*, 71(1), p. 16–22.

Avci, H., HassanİN, A., Hamouda, T., Kiliç, A., 2019. High performance fibers: A review on current state of art and future challenges. *Journal of Engineering and Architecture Faculty of Eskisehir Osmangazi University*, 27(2), p. 130–155.

Bae, J.-M., Kim, K.-N., Hattori, M., Hasegawa, K., Yoshinari, M., Kawada, E., Oda, Y., 2001. The flexural properties of fiber-reinforced composite with light-polymerized polymer matrix. *International Journal of Prosthodontics*, 14(1), p. 33–39.

Barbucci, R. 2002. Integrated biomaterials science, Springer Science & Business Media.

Başaran, E.G., Ayna, E., Vallittu, P.K., Lassila, L.V., 2013. Load bearing capacity of fiber-reinforced and unreinforced composite resin CAD/CAM-fabricated fixed dental prostheses. *Journal of Prosthetic Dentistry*, 109(2), p. 88–94.

Basavarajappa, S., Al-Kheraif, A.A., Elsharawy, M., Vallittu, P.K., 2016. Effect of solvent/disinfectant ethanol on the micro-surface structure and properties of multiphase denture base polymers. *Journal of the Mechanical Behavior of Biomedical Materials*, 54, p. 1–7.

Basavarajappa, S., Alkheraif, A.a.A., Alhijji, S.M., Matinlinna, J.P., Vallittu, P.K., 2017. Effect of ethanol treatment on mechanical properties of heat-polymerized polymethyl methacrylate denture base polymer. *Dental Materials Journal*, 36(6), p. 834–841.

Basavarajappa, S., Perea-Lowery, L., Aati, S., Al-Kheraif, A.A., Ramakrishnaiah, R., Matinlinna, J.P., Vallittu, P.K., 2019. The effect of ethanol on surface of semi-interpenetrating polymer network (IPN) polymer matrix of glass-fibre reinforced composite. *Journal of the Mechanical Behavior of Biomedical Materials*, 98, p. 1–10.

Beldüz Kara, N., Kanyilmaz, T., Çankaya, S., Kara, C., 2018. Evaluation of the effect of different post materials and adhesive systems on the bonding strength of short-post technique for primary teeth. *International Journal of Paediatric Dentistry*, 28(2), p. 239–248.

Bijelic-Donova, J., Keulemans, F., Vallittu, P.K., Lassila, L.V., 2020. Direct bilayered biomimetic composite restoration: The effect of a cusp-supporting short fiber-reinforced base design on the chewing fracture resistance and failure mode of molars with or without endodontic treatment. *Journal of the Mechanical Behavior of Biomedical Materials*, 103, p. 103554.

Bijelic-Donova, J., Garoushi, S., Lassila, L.V., Vallittu, P.K., 2015. Oxygen inhibition layer of composite resins: effects of layer thickness and surface layer treatment on the interlayer bond strength. *European Journal of Oral Sciences*, 123(1), p. 53–60.

Butterworth, C., Ellakwa, A.E., Shortall, A., 2003. Fibre-reinforced composites in restorative dentistry. *Dental Update*, 30(6), p. 300–306.

Cacciafesta, V., Sfondrini, M.F., Lena, A., Scribante, A., Vallittu, P.K., Lassila, L.V., 2008. Force levels of fiber-reinforced composites and orthodontic stainless steel wires: a 3-point bending test. *American Journal of Orthodontics and Dentofacial Orthopedics*, 133(3), p. 410–413.

Cadenaro, M., Antoniolli, F., Codan, B., Agee, K., Tay, F.R., Dorigo, E.D.S., Pashley, D.H., Breschi, L., 2010. Influence of different initiators on the degree of conversion of experimental adhesive blends in relation to their hydrophilicity and solvent content. *Dental Materials*, 26(4), p. 288–294.

Cadenaro, M., Breschi, L., Antoniolli, F., Navarra, C.O., Mazzoni, A., Tay, F.R., Di Lenarda, R., Pashley, D.H., 2008. Degree of conversion of resin blends in relation to ethanol content and hydrophilicity. *Dental Materials*, 24(9), p. 1194–1200.

Cauwels, R.G., Lassila, L.V., Martens, L.C., Vallittu, P.K., Verbeeck, R.M., 2014. Fracture resistance of endodontically restored, weakened incisors. *Dental Traumatology*, 30(5), p. 348–355.

Chen, S.Y., Liang, W.M., Yen, P.S., 2001. Reinforcement of acrylic denture base resin by incorporation of various fibers. *Journal of Biomedical Materials Research*, 58(2), p. 203–208.

Chen, W.-C., Lee, S.-J., Ho, B.-C., 1998. Diffusion coefficients of acrylic monomers in poly (methyl methacrylate). *Journal of Polymer Research*, 5(3), p. 187–191.

Clyne, T., Hull, D. 2019. An introduction to composite materials, Cambridge, UK, Cambridge University Press.

Conrad, H.J., Seong, W.-J., Pesun, I.J., 2007. Current ceramic materials and systems with clinical recommendations: a systematic review. *Journal of Prosthetic Dentistry*, 98(5), p. 389–404.

D'alpino, P.H.P., Vismara, M.V.G., González, A.H.M., De Oliveira Graeff, C.F., 2014. Free radical entrapment and crystallinity of resin composites after accelerated aging as a function of the expiration date. *Journal of the Mechanical Behavior of Biomedical Materials*, 36, p. 82–89.

Debnath, S., Wunder, S.L., Mccool, J.I., Baran, G.R., 2003. Silane treatment effects on glass/resin interfacial shear strengths. *Dental Materials*, 19(5), p. 441–448.

Deboer, J., Vermilyea, S., Brady, R., 1984. The effect of carbon fiber orientation on the fatigue resistance and bending properties of two denture resins. *Journal of Prosthetic Dentistry*, 51(1), p. 119–121.

Della Bona, A., Van Noort, R., 1995. Shear vs. tensile bond strength of resin composite bonded to ceramic. *Journal of Dental Research*, 74(9), p. 1591–1596.

Dewald, J., Ferracane, J., 1987. A comparison of four modes of evaluating depth of cure of light-activated composites. *Journal of Dental Research*, 66(3), p. 727–730.

Dj, L.S.F., Özcan, M., Krebs, E., Sandham, J., 2009. Adhesive properties of bonded orthodontic retainers to enamel: Stainless steel wire versus fiber-reinforced composites. *Jounal of Adhesive Dentistry*, 11(5), p. 381–390.

Drummond, J.L., 2008. Degradation, fatigue, and failure of resin dental composite materials. *Journal of Dental Research*, 87(8), p. 710–719.

Dyer, S.R., Lassila, L.V., Jokinen, M., Vallittu, P.K., 2004. Effect of fiber position and orientation on fracture load of fiber-reinforced composite. *Dental Materials*, 20(10), p. 947–955.

Edwards, K., 1998. An overview of the technology of fibre-reinforced plastics for design purposes. *Materials & Design*, 19(1-2), p. 1–10.

Ellakwa, A., Shortall, A., Shehata, M., Marquis, P., 2002a. Influence of bonding agent composition on flexural properties of an Ultra-High Molecular Weight Polyethylene Fiber-Reinforced Composite. *Operative Dentistry*, 27(2), p. 184–191.

Ellakwa, A.E., Shortall, A.C., Marquis, P.M., 2002b. Influence of fiber type and wetting agent on the flexural properties of an indirect fiber reinforced composite. *The Journal of Prosthetic Dentistry*, 88(5), p. 485–490.

Feinman, R., Smidt, A., 1997. A combination porcelain/fiber-reinforced composite bridge: a case report. *Practical Periodontics and Aesthetic Dentistry*, 9(8), p. 925–929.

Fráter, M.T., Sáry, T., Néma, V., Braunitzer, G., Vallittu, P.K., Lassila, L., Garoushi, S., 2020. Fatigue failure load of immature anterior teeth: influence of different fiber post-core systems. *Odontology*, 109(1), p. 222–230.

Gajewski, V.E., Pfeifer, C.S., Fróes-Salgado, N.R., Boaro, L.C., Braga, R.R., 2012. Monomers used in resin composites: degree of conversion, mechanical properties and water sorption/solubility. *Brazilian Dental Journal*, 23(5), p. 508–514.

Garoushi, S., Vallittu, P.K., 2007. Chairside fabricated fiber-reinforced composite fixed partial denture. *Libyan Journal of Medicine*, 2(1), p. 40–42.

Garoushi, S., Vallittu, P.K., Lassila, L., 2012. Effect of short fiber fillers on the optical properties of composite resins. *Journal of Materials Science Research*, 1(2), p. 174–180.

Garoushi, S., Vallittu, P.K., Watts, D.C., Lassila, L.V., 2008. Polymerization shrinkage of experimental short glass fiber-reinforced composite with semi-inter penetrating polymer network matrix. *Dental Materials*, 24(2), p. 211–215.

Garoushi, S.K., Lassila, L., Vallittu, P.K., 2006. Short fiber reinforced composite: the effect of fiber length and volume fraction. *Jounal of Contemporary Dental Practice*, 7(5), p. 10–17.

Garoushi, S.K., Lassila, L.V., Vallittu, P.K., 2007. Direct composite resin restoration of an anterior tooth: effect of fiber-reinforced composite substructure. *European Journal of Prosthodontics and Restorative Dentistry*, 15(2), p. 61–66.

Gibreel, M., Lassila, L.V., Närhi, T.O., Perea-Lowery, L., Vallittu, P.K., 2018. Load-bearing capacity of simulated Locator-retained overdenture system. *Journal of Prosthetic Dentistry*, 120(4), p. 558–564.

Gibreel, M., Lassila, L.V., Närhi, T.O., Perea-Lowery, L., Vallittu, P.K., 2019. Fatigue resistance of a simulated single locator overdenture system. *Journal of Prosthetic Dentistry*, 122(6), p. 557–563.

Goldberg, A., Burstone, C., 1992. The use of continuous fiber reinforcement in dentistry. *Dental Materials*, 8(3), p. 197–202.

Goldberg, A.J., Burstone, C.J., Hadjinikolaou, I., Jancar, J., 1994. Screening of matrices and fibers for reinforced thermoplastics intended for dental applications. *Journal of Biomedical Materials Research*, 28(2), p. 167–173.

Grave, A., Chandler, H., Wolfaardt, J., 1985. Denture base acrylic reinforced with high modulus fibre. *Dental Materials*, 1(5), p. 185–187.

Gutteridge, D., 1992. Reinforcement of poly (methyl methacrylate) with ultra-high-modulus polyethylene fibre. *Journal of Dentistry*, 20(1), p. 50–54.

Hamza, T.A., Rosenstiel, S.F., Elhosary, M.M., Ibraheem, R.M., 2004. The effect of fiber reinforcement on the fracture toughness and flexural strength of provisional restorative resins. *Journal of Prosthetic Dentistry*, 91(3), p. 258–264.

Heikkinen, T., Matinlinna, J., Vallittu, P., Lassila, L., 2013. Long term water storage deteriorates bonding of composite resin to alumina and zirconia short communication. *Open Dentistry Journal*, 7, p. 123–125.

Huang, X., 2009. Fabrication and properties of carbon fibers. *Materials*, 2(4), p. 2369–2403.

Ikeda, T., De Munck, J., Shirai, K., Hikita, K., Inoue, S., Sano, H., Lambrechts, P., Van Meerbeek, B., 2005. Effect of evaporation of primer components on ultimate tensile strengths of primer–adhesive mixture. *Dental Materials*, 21(11), p. 1051–1058.

Ilday, N., Seven, N., 2011. The influence of different fiber-reinforced composites on shear bond strengths when bonded to enamel and dentin structures. *Journal of Dental Sciences*, 6(2), p. 107–115.

Inami, T., Tanimoto, Y., Minami, N., Yamaguchi, M., Kasai, K., 2015. Color stability of laboratory glass-fiber-reinforced plastics for esthetic orthodontic wires. *Korean Journal of Orthodontics*, 45(3), p. 130–135.

Jancar, J., Dibenedetto, A., 1993. Fibre reinforced thermoplastic composites for dentistry. *Journal of Materials Science: Materials in Medicine*, 4(6), p. 555–561.

Jassal, M., Ghosh, S., 2002. Aramid fibres-An overview. *Indian Journal of Fibre & Textile Research*, 27, p. 290–306.

Jiang, B., Liu, C., Zhang, C., Wang, B., Wang, Z., 2007. The effect of non-symmetric distribution of fiber orientation and aspect ratio on elastic properties of composites. *Composites Part B: Engineering*, 38(1), p. 24–34.

John, J., Gangadhar, S.A., Shah, I., 2001. Flexural strength of heat-polymerized polymethyl methacrylate denture resin reinforced with glass, aramid, or nylon fibers. *Journal of Prosthetic Dentistry*, 86(4), p. 424–427.

Kalantar, J., Drzal, L., 1990. The bonding mechanism of aramid fibres to epoxy matrices. *Journal of Materials Science*, 25(10), p. 4186–4193.

Kallio, T., Lastumäki, T., Vallittu, P., 2001. Bonding of restorative and veneering composite resin to somepolymeric composites. *Dental Materials*, 17(1), p. 80–86.

Kallio, T., Lastumäki, T., Vallittu, P., 2003. Effect of resin application time on bond strength of polymer substrate repaired with particulate filler composite. *Journal of Materials Science: Materials in Medicine*, 14(11), p. 999–1004.

Kallio, T.T., Lastumäki, T.M., Lassila, L.V., Vallittu, P.K., 2014. Influence of intermediate resin on the bond strength of light-curing composite resin to polymer substrate. *Acta Odontologica Scandinavica*, 72(3), p. 202–208.

Karmaker, A., T Dibenedetto, A., Goldberg, A., 1997. Extent of conversion and its effect on the mechanical performance of Bis-GMA/PEGDMA-based resins and their composites with continuous glass fibres. *Journal of Materials Science: Materials in Medicine*, 8(6), p. 369–374.

Kawaguchi, T., Lassila, L.V., Tokue, A., Takahashi, Y., Vallittu, P.K., 2011a. Influence of molecular weight of polymethyl (methacrylate) beads on the properties and structure of cross-linked denture base polymer. *Journal of the Mechanical Behavior of Biomedical Materials*, 4(8), p. 1846–1851.

Kawaguchi, T., Lassila, L.V., Vallittu, P.K., Takahashi, Y., 2011b. Mechanical properties of denture base resin cross-linked with methacrylated dendrimer. *Dental Materials*, 27(8), p. 755–761.

Khan, A.A., Al-Kheraif, A.A., Al-Shehri, A.M., Säilynoja, E., Vallittu, P.K., 2018a. Polymer matrix of fiber-reinforced composites: Changes in the semi-interpenetrating polymer network during the shelf life. *Journal of the Mechanical Behavior of Biomedical Materials*, 78, p. 414–419.

Khan, A.A., Al-Kheraif, A.A., Mohamed, B.A., Perea-Lowery, L., Säilynoja, E., Vallittu, P.K., 2018b. Influence of primers on the properties of the adhesive interface between resin composite luting cement and fiber-reinforced composite. *Journal of the Mechanical Behavior of Biomedical Materials*, 88, p. 281–287.

Khan, A.A., Al Kheraif, A., Jamaluddin, S., Elsharawy, M., Divakar, D.D., 2017a. Recent trends in surface treatment methods for bonding composite cement to zirconia: a review. *Journal of Adhesive Dentistry*, 19(1), p. 7–19.

Khan, A.A., Al Kheraif, A.A., Alhijji, S.M., Matinlinna, J.P., 2016. Effect of grit-blasting air pressure on adhesion strength of resin to titanium. *International Journal of Adhesion and Adhesives*, 65, p. 41–46.

Khan, A.A., Al Kheraif, A.A., Syed, J., Divakar, D.D., Matinlinna, J.P., 2018c. Enhanced resin zirconia adhesion with carbon nanotubes-infused silanes: A pilot study. *The Journal of Adhesion*, 94(3), p. 167–180.

Khan, A.A., Mirza, E.H., Syed, J., Al-Khureif, A.A., Mehmood, A., Vallittu, P.K., Alfotawi, R., 2017b. Single and multi-walled carbon nanotube fillers in poly (methyl methacrylate)-based implant material. *Journal of Biomaterials and Tissue Engineering*, 7(9), p. 798–806.

Khan, A.A., Mohamed, B.A., Al-Shamrani, S.S., Ramakrishnaiah, R., Perea-Lowery, L., Säilynoja, E., Vallittu, P.K., 2019. Influence of monomer systems on the bond strength between resin composites and polymerized fiber-reinforced composite upon aging. *Journal of Adhesive Dentistry*, 21, p. 509–516.

Khan, A.S., Azam, M.T., Khan, M., Mian, S.A., Rehman, I.U., 2015. An update on glass fiber dental restorative composites: a systematic review. *Materials Science and Engineering C*, 47, p. 26–39.

Khan, A.S., Khalid, H., Sarfraz, Z., Khan, M., Iqbal, J., Muhammad, N., Fareed, M.A. Rehman, I.U., 2017c. Vibrational spectroscopy of selective dental restorative materials. *Applied Spectroscopy Reviews*, 52(6), p. 507–540.

Khan, S.I.R., Ramachandran, A., Alfadley, A., Baskaradoss, J.K., 2018d. Ex vivo fracture resistance of teeth restored with glass and fiber reinforced composite resin. *Journal of the Mechanical Behavior of Biomedical Materials*, 82, p. 235–238.

Kilponen, L., Uusitalo, E., Tolvanen, M., Varrela, J., Vallittu, P., 2016. Photopolymerization of light curing adhesives used with metal orthodontic brackets and matrices. *Journal of Biomaterials and Tissue Engineering*, 6(8), p. 659–664.

Kilponen, L., Varrela, J., Vallittu, P.K., 2019. Priming and bonding metal, ceramic and polycarbonate brackets. *Biomaterial Investigations in Dentistry*, 6(1), p. 61–72.

Kim, H.S., Hong, S.I., Kim, S.J., 2001. On the rule of mixtures for predicting the mechanical properties of composites with homogeneously distributed soft and hard particles. *Journal of Materials Processing Technology*, 112(1), p. 109–113.

Kim, J.-K., Mai, Y.-W. 1998. Engineered interfaces in fiber reinforced composites, Elsevier.

Kolbeck, C., Rosentritt, M., Behr, M., Lang, R., Handel, G., 2002. In vitro examination of the fracture strength of 3 different fiber-reinforced composite and 1 all-ceramic posterior inlay fixed partial denture systems. *Journal of Prosthodontics*, 11(4), p. 248–253.

Kumar, A., Tekriwal, S., Rajkumar, B., Gupta, V., Rastogi, R., 2016. A review on fibre reinforced composite resins. *Annals of Prosthodontics and Restorative Dentistry*, 2(4), p. 11–16.

Kuusisto, N., Vallittu, P., Lassila, L., Huumonen, S., 2015. Evaluation of intensity of artefacts in CBCT by radio-opacity of composite simulation models of implants in vitro. *Dentomaxillofacial Radiology*, 44(2), p. 20140157.

Landel, R.F., Nielsen, L.E. 1993. Mechanical properties of polymers and composites, CRC press.

Larson, W.R., Dixon, D.L., Aquilino, S.A., Clancy, J.M., 1991. The effect of carbon graphite fiber reinforcentent on the strength of provisional crown and fixed partial denture resins. *Journal of Prosthetic Dentistry*, 66(6), p. 816–820.

Lastumäki, T., Kallio, T., Vallittu, P., 2002. The bond strength of light-curing composite resin to finally polymerized and aged glass fiber-reinforced composite substrate. *Biomaterials*, 23(23), p. 4533–4539.

Lastumäki, T., Lassila, L., Vallittu, P., 2003. The semi-interpenetrating polymer network matrix of fiber-reinforced composite and its effect on the surface adhesive properties. *Journal of Materials Science: Materials in Medicine*, 14(9), p. 803–809.

Le Bell-Rönnlöf, A.-M., Lassila, L.V., Kangasniemi, I., Vallittu, P.K., 2011. Load-bearing capacity of human incisor restored with various fiber-reinforced composite posts. *Dental Materials*, 27(6), p. e107–e115.

Le Bell, A.-M., Lassila, L.V., Kangasniemi, I., Vallittu, P.K., 2005. Bonding of fibre-reinforced composite post to root canal dentin. *Journal of Dentistry*, 33(7), p. 533–539.

Le Bell, A.-M., Tanner, J., Lassila, L.V., Kangasniemi, I., Vallittu, P.K., 2004. Bonding of composite resin luting cement to fiber-reinforced composite root canal posts. *Journal of Adhesive Dentistry*, 6(4), p. 319–325.

Li, H.Y., Chen, Y.Y., Zhu, F.F., Li, C.W., 2014. Unsaturated polyesters with pendant double bonds and Investigation of their self curable activity. *Advanced Materials Research*, 1052, 262–269.

Lindblad, R.M., Lassila, L.V., Salo, V., Vallittu, P.K., Tjäderhane, L., 2010. Effect of chlorhexidine on initial adhesion of fiber-reinforced post to root canal. *Journal of Dentistry*, 38(10), p. 796–801.

Liu, Q., Ding, J., Chambers, D.E., Debnath, S., Wunder, S.L., Baran, G.R., 2001. Filler-coupling agent-matrix interactions in silica/polymethylmethacrylate composites. *Journal of Biomedical Materials Research*, 57(3), p. 384–393.

Lucchese, A., Manuelli, M., Ciuffreda, C., Albertini, P., Gherlone, E., Perillo, L., 2018. Comparison between fiber-reinforced polymers and stainless steel orthodontic retainers. *Korean Journal of Orthodontics*, 48(2), p. 107–112.

Mangoush, E., Säilynoja, E., Prinssi, R., Lassila, L., Vallittu, P.K., Garoushi, S., 2017. Comparative evaluation between glass and polyethylene fiber reinforced composites: A review of the current literature. *Journal of Clinical and Experimental Dentistry*, 9(12), p. e1408–e1417.

Mannocci, F., Sherriff, M., Watson, T., Vallittu, P., 2005. Penetration of bonding resins into fibre-reinforced composite posts: a confocal microscopic study. *International Endodontic Journal*, 38(1), p. 46–51.

Masete, M.S., Muchavi, N.S., Chikosha, S. The effect of specimen geometry on tensile properties of titanium alloy metal sheet. IOP Conference Series: Materials Science and Engineering, 23–28 October 2018 South Africa. IOP Publishing, 012015.

Matinlinna, J.P., Lassila, L.V., Özcan, M., Yli-Urpo, A., Vallittu, P.K., 2004. An introduction to silanes and their clinical applications in dentistry. *International Journal of Prosthodontics*, 17(2), p. 155–164.

Mccabe, J., Wilson, H., 1974. Polymers in dentistry. *Journal of Oral Rehabilitation*, 1(4), p. 335–351.

Müller, J.A., Rohr, N., Fischer, J., 2017. Evaluation of ISO 4049: water sorption and water solubility of resin cements. *European Journal of Oral Sciences*, 125(2), p. 141–150.

Murphy, J. 1998. The reinforced plastics handbook, Elsevier Science.

Narva, K.K., Lassila, L.V., Vallittu, P.K., 2005a. Flexural fatigue of denture base polymer with fiber-reinforced composite reinforcement. *Composites Part A: Applied Science and Manufacturing*, 36(9), p. 1275–1281.

Narva, K.K., Lassila, L.V., Vallittu, P.K., 2005b. The static strength and modulus of fiber reinforced denture base polymer. *Dental Materials*, 21(5), p. 421–428.

Narva, K.K., Vallittu, P.K., Helenius, H., Yli-Urpo, A., 2001. Clinical survey of acrylic resin removable denture repairs with glass-fiber reinforcement. *International Journal of Prosthodontics*, 14(3).

Nasirzadeh, K., Zimin, D., Neueder, R., Kunz, W., 2004. Vapor-pressure measurements of liquid solutions at different temperatures: Apparatus for use over an extended temperature range and some new data. *Journal of Chemical and Engineering Data*, 49(3), p. 607–612.

Nihi, F.M., Fabre, H.S.C., Garcia, G., Fernandes, K.B.P., Ferreira, F.B.D.A., Wang, L., 2009. In vitro assessment of solvent evaporation from commercial adhesive systems compared to experimental systems. *Brazilian Dental Journal*, 20(5), p. 396–402.

Oberholzer, T., Pitout, E., Lombard, R., Du Preez, I., 2007. Effect of woven glass fibre reinforcement on the flexural strength of composites: scientific. *South African Dental Journal*, 62(9), p. 386–389.

Obukuro, M., Takahashi, Y., Shimizu, H., 2008. Effect of diameter of glass fibers on flexural properties of fiber-reinforced composites. *Dental Materials Journal*, 27(4), p. 541–548.

Ohtonen, J., Vallittu, P., Lassila, L., 2013. Effect of monomer composition of polymer matrix on flexural properties of glass fibre-reinforced orthodontic archwire. *European Journal of Orthodontics*, 35(1), p. 110–114.

Özcan, M., Van Der Sleen, J.M., Kurunmäki, H., Vallittu, P.K., 2006. Comparison of repair methods for ceramic-fused-to-metal crowns. *Journal of Prosthodontics*, 15(5), p. 283–288.

Perea, L., Matinlinna, J.P., Tolvanen, M., Lassila, L.V., Vallittu, P.K., 2014. Fiber-reinforced composite fixed dental prostheses with various pontics. *Journal of Adhesive Dentistry*, 16(2), p. 161–168.

Perea, L., Matinlinna, J.P., Tolvanen, M., Mannocci, F., Watson, T.F., Vallittu, P.K., 2015. Penetration depth of monomer systems into acrylic resin denture teeth used as pontics. *The Journal of Prosthetic Dentistry*, 113(5), p. 480–487.

Perrin, P., Meyer-Lueckel, H., Wierichs, R., 2020. Longevity of immediate rehabilitation with direct fiber reinforced composite fixed partial dentures after up to 9 years. *Journal of Dentistry*, 100, p. 103438.

Pradhan, S., Lach, R., Le, H.H., Grellmann, W., Radusch, H.-J., Adhikari, R., 2013. Effect of filler dimensionality on mechanical properties of nanofiller reinforced polyolefin elastomers. *ISRN Polymer Science*, 2013.

Rasmussen, S., 1996. Analysis of dental shear bond strength tests, shear or tensile? *International Journal of Adhesion and Adhesives*, 16(3), p. 147–154.

Rosato, D.V., Rosato, D.V. 2004. Reinforced plastics handbook, Elsevier Science.

Ruyter, I., Ekstrand, K., Björk, N., 1986. Development of carbon/graphite fiber reinforced poly (methyl methacrylate) suitable for implant-fixed dental bridges. *Dental Materials*, 2(1), p. 6–9.

Ruyter, I.E., 1982. Methacrylate-based polymeric dental materials: Conversion and related properties: summary and review. *Acta Odontologica Scandinavica*, 40(5), p. 359–376.

Ruyter, I.E., Svendsen, S.A., 1980. Flexural properties of denture base polymers. *Journal of Prosthetic Dentistry*, 43(1), p. 95–104.

Sattler, K.D. 2010. Handbook of Nanophysics: Functional Nanomaterials, CRC press.

Schreiber, C., 1974. The clinical application of carbon fibre/polymer denture bases. *British Dental Journal*, 137(1), p. 21–22.

Scribante, A., Vallittu, P.K., Özcan, M., 2018a. Fiber-reinforced composites for dental applications. *BioMed Research International*, 2018.

Scribante, A., Vallittu, P.K., Özcan, M., Lassila, L.V., Gandini, P., Sfondrini, M.F., 2018b. Travel beyond clinical uses of fiber reinforced composites (FRCs) in dentistry: a review of past employments, present applications, and future perspectives. *BioMed Research International*, 2018.

Segerström, S., Meriç, G., Knarvang, T., Ruyter, I.E., 2005. Evaluation of two matrix materials intended for fiber-reinforced polymers. *European Journal of Oral Sciences*, 113(5), p. 422–428.

Sfondrini, M., Calderoni, G., Vitale, M., Gandini, P., Scribante, A., 2018. Is laser conditioning a valid alternative to conventional etching for aesthetic brackets. *European Journal of Paediatric Dentistry*, 19(1), p. 61–66.

Shinya, M., Shinya, A., Lassila, L.V., Gomi, H., Varrela, J., Vallittu, P.K., Shinya, A., 2008. Treated enamel surface patterns associated with five orthodontic adhesive systems—surface morphology and shear bond strength. *Dental Materials Journal*, 27(1), p. 1–6.

Smith, D., 1962. Recent developments and prospects in dental polymers. *The Journal of Prosthetic Dentistry*, 12(6), p. 1066–1078.

Sperling, L. 1981. An introduction to polymer networks and IPNs. In: Sperling, L. (ed.) Interpenetrating polymer networks and related materials. New York , USA: Springer.

Strassler, H.E., Serio, C.L., 2007. Esthetic considerations when splinting with fiber-reinforced composites. *Dental Clinics of North America*, 51(2), p. 507–524.

Tanimoto, Y., Inami, T., Yamaguchi, M., Nishiyama, N., Kasai, K., 2015. Preparation, mechanical, and in vitro properties of glass fiber-reinforced polycarbonate composites for orthodontic application. *Journal of Biomedical Materials Research Part B: Applied Biomaterials*, 103(4), p. 743–750.

Tanner, J., Le Bell-Rönnlöf, A.-M., Vallittu, P. 2017. Root canal anchoring systems. A clinical guide to fibre reinforced composites (frcs) in dentistry. Elsevier.

Tayab, T., Vizhi, K., Srinivasan, I., 2011. Space maintainer using fiber-reinforced composite and natural tooth–a non-invasive technique. *Dental Traumatology*, 27(2), p. 159–162.

Thomason, J., 2019. Glass fibre sizing: A review. *Composites Part A: Applied Science and Manufacturing*, 127, p. 105619.

Ute, K., Yamasaki, Y., Naito, M., Miyatake, N., Hatada, K., 1995. Controlled synthesis of isotactic and symmetrical poly (methyl methacrylate) directed toward uniform polymers with high crystallinity. *Polymer Journal*, 27(9), p. 951–958.

Uzun, G., Hersek, N., Tincer, T., 1999. Effect of five woven fiber reinforcements on the impact and transverse strength of a denture base resin. *Journal of Prosthetic Dentistry*, 81(5), p. 616–620.

Uzun, G., Keyf, F., 2003. The effect of fiber reinforcement type and water storage on strength properties of a provisional fixed partial denture resin. *Journal of Biomaterials Applications*, 17(4), p. 277–286.

Vallittu, P., 1995a. The effect of void space and polymerization time on transverse strength of acrylic-glass fibre composite. *Journal of Oral Rehabilitation*, 22(4), p. 257–261.

Vallittu, P., 1997a. Curing of a silane coupling agent and its effect on the transverse strength of autopolymerizing polymethylmethacrylate—glass fibre composite. *Journal of Oral Rehabilitation*, 24(2), p. 124–130.

Vallittu, P. Strength and interfacial adhesion of FRC-tooth system. The second international symposium on fiber-reinforced plastics in dentistry, 2001 Nijmegen, The Netherlands.

Vallittu, P., 2002. Use of woven glass fibres to reinforce a composite veneer. A fracture resistance and acoustic emission study. *Journal of Oral Rehabilitation*, 29(5), p. 423–429.

Vallittu, P., Lassila, V., 1992. Reinforcement of acrylic resin denture base material with metal or fibre strengtheners. *Journal of Oral Rehabilitation*, 19(3), p. 225–230.

Vallittu, P., Matinlinna, J. 2017. Types of FRCs used in dentistry. A Clinical Guide to Fibre Reinforced Composites (FRCs) in Dentistry. Elsevier.

Vallittu, P., Özcan, M. 2017. Clinical Guide to Principles of Fiber-Reinforced Composites in Dentistry, Woodhead Publishing.

Vallittu, P.K., 1994. Acrylic resin-fiber composite—Part II: The effect of polymerization shrinkage of polymethyl methacrylate applied to fiber roving on transverse strength. *Journal of Prosthetic Dentistry*, 71(6), p. 613–617.

Vallittu, P.K., 1995b. Impregnation of glass fibres with polymethylmethacrylate using a powder-coating method. *Applied Composite Materials*, 2(1), p. 51–58.

Vallittu, P.K., 1996. A review of fiber-reinforced denture base resins. *Journal of Prosthodontics*, 5(4), p. 270–276.

Vallittu, P.K., 1997b. Ultra-high-modulus polyethylene ribbon as reinforcement for denture polymethyl methacrylate: a short communication. *Dental Materials*, 13(5-6), p. 381–382.

Vallittu, P.K., 1999. Flexural properties of acrylic resin polymers reinforced with unidirectional and woven glass fibers. *Journal of Prosthetic Dentistry*, 81(3), p. 318–326.

Vallittu, P.K., 2009. Interpenetrating polymer networks (IPNs) in dental polymers and composites. *Journal of Adhesion Science and Technology*, 23(7-8), p. 961–972.

Vallittu, P.K., 2015. High-aspect ratio fillers: fiber-reinforced composites and their anisotropic properties. *Dental Materials*, 31(1), p. 1–7.

Vallittu, P.K., 2017. Bioactive glass-containing cranial implants: an overview. *Journal of Materials Science*, 52(15), p. 8772–8784.

Vallittu, P.K., 2018. An overview of development and status of fiber-reinforced composites as dental and medical biomaterials. *Acta Biomaterialia Odontologica Scandinavica*, 4(1), p. 44–55.

Van Noort, R., Barbour, M. 2014. Introduction to Dental Materials-E-Book, Elsevier Health Sciences.

Varley, D., Yousaf, S., Youseffi, M., Mozafari, M., Khurshid, Z., Sefat, F. 2019. Fiber-reinforced composites. Advanced Dental Biomaterials. Elsevier.

Vivaldo-Lima, E., Saldívar-Guerra, E. 2013. Handbook of polymer synthesis, characterization, and processing, Wiley Online Library.

Vuorinen, A.-M., Dyer, S.R., Lassila, L.V., Vallittu, P.K., 2008. Effect of rigid rod polymer filler on mechanical properties of poly-methyl methacrylate denture base material. *Dental Materials*, 24(5), p. 708–713.

Vuorinen, A.-M., Dyer, S.R., Lassila, L.V., Vallittu, P.K., 2011a. Bonding of BisGMA–TEGDMA-resin to bulk poly (paraphenylene) based rigid rod polymer. *Composite Interfaces*, 18(5), p. 387–398.

Vuorinen, A.-M., Dyer, S.R., Vallittu, P.K., Lassila, L.V., 2011b. Effect of water storage on the microtensile bond strength of composite resin to dentin using experimental rigid rod polymer modified primers. *Journal of Adhesive Dentistry*, 13(4), p. 333–340.

Xu, Z., Gao, C., 2015. Graphene fiber: a new trend in carbon fibers. *Materials Today*, 18(9), p. 480–492.

Yazdanie, N., Mahood, M., 1985. Carbon fiber acrylic resin composite: an investigation of transverse strength. *Journal of Prosthetic Dentistry*, 54(4), p. 543–547.

Zhang, D., He, M., Qin, S., Yu, J., 2017. Effect of fiber length and dispersion on properties of long glass fiber reinforced thermoplastic composites based on poly (butylene terephthalate). *RSC Advances*, 7(25), p. 15439–15454.

Zhang, M., Matinlinna, J.P., 2012. E-glass fiber reinforced composites in dental applications. *Silicon*, 4(1), p. 73–78.

TURUN
YLIOPISTO
UNIVERSITY
OF TURKU

Painosalama Oy, Turku, Finland 2021

ISBN 978-951-29-8404-6 (PRINT)
ISBN 978-951-29-8405-3 (PDF)
ISSN 0355-9483 (Print)
ISSN 2343-3213 (Online)